

University of Arkansas, Fayetteville  
**ScholarWorks@UARK**

---

Graduate Theses and Dissertations

---

12-2014

## Designing Magnetically Responsive Ultrafiltration Membranes

Robert William Dong  
*University of Arkansas, Fayetteville*

Follow this and additional works at: <https://scholarworks.uark.edu/etd>



Part of the [Polymer Chemistry Commons](#), and the [Polymer Science Commons](#)

---

### Citation

Dong, R. W. (2014). Designing Magnetically Responsive Ultrafiltration Membranes. *Graduate Theses and Dissertations* Retrieved from <https://scholarworks.uark.edu/etd/2104>

This Thesis is brought to you for free and open access by ScholarWorks@UARK. It has been accepted for inclusion in Graduate Theses and Dissertations by an authorized administrator of ScholarWorks@UARK. For more information, please contact [scholar@uark.edu](mailto:scholar@uark.edu), [uarepos@uark.edu](mailto:uarepos@uark.edu).

## Designing Magnetically Responsive Ultrafiltration Membranes

# Designing Magnetically Responsive Ultrafiltration Membranes

A thesis submitted in partial fulfillment  
of the requirements for the degree of  
Master of Science in Chemical Engineering

by

Robert Dong  
University of Colorado  
Bachelor of Science in Chemical and Biological Engineering, 2012

December 2014  
University of Arkansas

This thesis is approved for recommendation to the Graduate Council.

---

Dr. Ranil Wickramasinghe  
Thesis Director

---

Dr. Xianghong Qian  
Committee Member

---

Dr. Paul Millett  
Committee Member

---

Dr. Mathias Ulbricht  
Committee Member

## **Abstract**

Ultrafiltration (UF) membranes developed out of a need for protein separation processes. Currently, they are used in a variety of industries ranging from food manufacturing to pharmaceuticals for two main purposes: concentration, separation, and buffer exchange. UF membrane processes in product streams undergo frequent use and like all membrane processes experience a gradual decline in performance due to fouling phenomena both irreversible and reversible. Ultimately, performance declines to a point where the UF membrane needs to be replaced. Frequent replacement of UF membranes is detrimental to major industries that require high product throughput using UF processes. Thus, it is important to try and overcome any type of fouling to reduce the decline in UF membrane performance and thereby limit the frequency of UF replacement. One of the novel ways to do this is to design membranes that respond to changes in their environment or “responsive” membranes. Magnetically responsive membranes are a small emerging subset of the investigations in this field. The work in this thesis attempts to expand the knowledge of magnetically responsive membranes and apply it to UF membranes. Successful surface modification with magnetite ( $\text{Fe}_3\text{O}_4$ ) nanoparticle capped poly(hydroxyl ethyl methacrylate) chains of UF regenerated cellulose membranes was confirmed by atomic force microscopy (AFM) and X-ray photospectroscopy (XPS) surface characterization methods. However, measuring the responsive nature of modified UF membranes resulted in inconclusive results. Possible reasons include the chemical modification method with regards to polymer chain density and length, reducing possible oxidation for reaction control, and addressing multiple amine attachment sites on the nanoparticle. Further investigations and studies are needed moving forward.

## Table of Contents

1.	Introduction.....	1
2.	Background.....	4
2.1	Modification of Membrane Surface Properties .....	4
2.2	Stimulus Responsive Membranes.....	8
2.3	Temperature Responsive Membranes .....	9
2.4	pH Responsive Membranes .....	10
2.5	Magnetic Responsive Membranes.....	10
3.	Experimental.....	14
3.1	Membrane Modification.....	14
3.2	Surface Characterization.....	17
3.3	Flux Measurements.....	18
3.4	Dextran Rejection.....	19
4.	Results.....	21
4.1	Surface Characterization.....	21
4.2	Flux Measurements.....	25
4.3	Dextran Rejection.....	28
5.	Discussion.....	33
5.1	Surface Characterization.....	33
5.2	Flux Measurements.....	33

5.3	Dextran Rejection .....	35
6.	Conclusion .....	37
7.	Works Cited .....	38
8.	Appendices.....	42

## Table of Figures

Figure 1: Acting forces in determining the thickness of concentration polarization. ....	2
Figure 2: Schematic Representation of the ATRP reaction. ....	7
Table 1: Examples of stimulus responsive polymers that lists the external stimulus, the membrane matrix material, and modification method. ....	8
Figure 3: Diagram of chemistry used to modify UF RC membranes. ....	15
Table 2: Dextran fraction concentrations as adapted from Zydney et al. <sup>43</sup> ....	20
Figure 4: XPS carbon peak diagrams for the unmodified membrane, after ATRP polymerization, and after the monomer addition reaction. ....	22
Figure 5: XPS iron peak diagrams for the unmodified membrane and NP modified membrane .	22
Figure 6: XPS nitrogen peak diagrams for the unmodified membrane and the NP modified membrane. ....	23
Figure 7: AFM images of unmodified membrane (A), poly(HEMA) modified membrane (B), and the NP modified membrane (C). ....	24
Figure 8: SEM images of the unmodified membrane surface at 25,000x and 50,000x (A and B) and the nanoparticle modified surface at 25,000x and 50,000x (C and D). ....	25
Figure 9: DI Water Flux measurements for different stages of modification. Values are an average out of 5 and the error bars represent the standard deviation. ....	26
Figure 10: Rejection of BSA for different modified membranes. Error bars represent the uncertainty in the measurements as propagated through the calculations. ....	27
Table 3: Legend for membrane labels in Figure 10. ....	28
Figure 11: Dextran HPLC chromatogram for the 1 hr ATRP - NP modified membrane. ....	29

Figure 12: Rejection vs. MW curve used to determine MWCO for 1 hr ATRP - NP modified membrane.....	30
Figure 13: MWCO for modified membranes of different conditions. The values were an average of three measurements and the error bars represent the standard deviation. ....	30
Figure 14: Summary of HPLC chromatogram signals from individual dextran fractions and the combined dextran challenge solutions. ....	31
Figure 15: Comparison of dextran challenge solution and additive signal of individual dextran fractions.....	31
Figure 16: Calibration curve used to correlate MW (Da) of dextran with elution time (min). ....	32
Figure 17: Operating Pressure (psi) vs. Flux (LMH) that was used to determine the critical pressure and the best operating pressure for the 0.1 g/L BSA filtration experiments. ....	42
Figure 18: Dextran HPLC chromatogram for the 1 hour ATRP modified membrane. ....	42
Figure 19: Dextran HPLC chromatogram for the 30 min ATRP - NP modified membrane. ....	43
Figure 20: Dextran HPLC chromatogram for the 30 min hr ATRP without NP modified membrane.....	43
Figure 21: Rejection vs. MW curve used to determine MWCO for 1 hr ATRP without NP modified membrane. ....	44
Figure 22: Rejection vs. MW curve used to determine MWCO for 30 minute ATRP without NP modified membrane. ....	44
Figure 23: Rejection vs. MW curve used to determine MWCO for 30 minute ATRP - NP modified membrane. ....	45



## 1. Introduction

On the most fundamental level, membranes are barriers that stabilize an interface between two bulk fluids. This very general definition encompasses everything from biological membranes to synthetic membranes. When applied in chemical engineering, synthetic membranes are most often utilized in a variety of unit operations that focus on separation processes. Based on the desired particle size to be separated, membranes fall into four categories: microfiltration (MF), ultrafiltration (UF), nanofiltration (NF), and reverse osmosis (RO). The focus of this project will be on UF membranes. UF membranes fall in a pore size range between MF and NF membranes (100 nm to 1  $\mu\text{m}$ ). Typically, UF membranes are used to separate particles that fall in the range of .5 to 500 kDa, which include proteins, viruses, tobacco smoke, colloidal silica, gelatin, large endotoxins, etc.

In addition, UF unit operations are run in tangential filtration mode with transmembrane pressures that range from 2 – 10 bar.<sup>2</sup> Thus, UF can be used for a variety of separation processes which include, but are not limited to virus filtration, therapeutic protein polishing, juice concentration, whey separation, wastewater treatment, and paper production.<sup>3-5</sup> The widespread use of UF membranes and membranes in general are due to its relatively low operating cost, high selectivity, relatively mild operating conditions (no changes in ionic strength and temperature), and easy scale-up.<sup>5,6</sup>

For all the advantages of using UF and membrane processes, major drawbacks hinder a larger application of membrane processes as a tool to solve problems in chemical engineering. Similar to most separation processes, the goal is to maximize solute rejection and permeate flow and maintain this performance for as long as possible.<sup>7</sup> Unfortunately, all UF and membrane

processes will suffer a decline in separation performance until they must be cleaned or replaced. The two largest factors for this performance decline are concentration polarization and fouling.<sup>8</sup>

Concentration polarization is due to the development of a high concentration solute region near the membrane surface. This region is caused by convection of rejected species to the membrane surface and its thickness is dictated by a counteracting back diffusion of solutes from the high concentration region to the bulk feed as illustrated in Figure 1.<sup>7</sup> Due to the increased viscosity and osmotic pressure created by the high concentration region, membrane processes will experience a subsequent drop in flux and an apparent decrease in rejection.<sup>2</sup> Concentration polarization can lead to or is usually accompanied by fouling of the membrane.

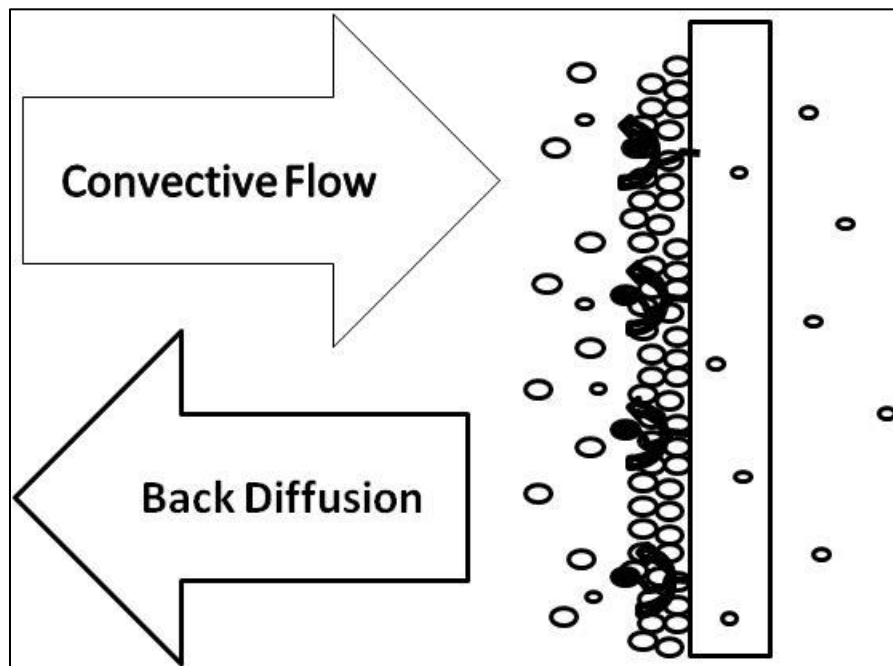


Figure 1: Acting forces in determining the thickness of concentration polarization.

Fouling of the membrane causes a drop in flux associated with the combined effect of physical, chemical, and biological factors. Examples of these interactions include, but are not limited to, physical blockage of pores, development of a physical cake layer, adsorption of proteins due to electrostatic interactions with the membrane surface, and chemical bonding of

solutes to the membrane surface.<sup>9</sup> These interactions increase with a longer residence time near the surface, which is why concentration polarization usually leads to and/or accompanies fouling. Flux decline due to fouling may be regenerated by cleaning the membrane, but irreversible fouling will lead to eventual membrane replacement.<sup>8</sup> The root cause of fouling is due to adsorption of unwanted species on the membrane surface. Some examples of fouling phenomenon include adsorption of solutes, clogging of membrane pores, cake layer compaction, bacterial growth, and gel layer formation.<sup>9</sup>

In order to reduce concentration polarization and fouling a number of approaches have been taken, which include changing membrane properties, changing the properties of the feed, and modifying the filtration operating conditions.<sup>9,10</sup> However, the discovery of stimulus responsive polymers and their incorporation into membranes has provided another way to reduce concentration polarization and fouling.<sup>6,11</sup> A recent study, explored this concept by using Fe<sub>3</sub>O<sub>4</sub> superparamagnetic nanoparticle (NP) capped polymers to reduce concentration polarization effects.<sup>12</sup> This thesis is an extension of the aforementioned study and will attempt to reduce concentration polarization effects for regenerated cellulose (RC) UF membranes. There are three stages to the thesis: successful attachment of NP capped polymers to the membrane surface, characterizing the membrane, and finally determining the effect of the modified membrane.

## 2. Background

As stated in the introduction, this thesis aims to reduce concentration polarization effects for RC UF membranes. The approach will be to create a stimulus responsive membrane. In a simple definition, stimulus responsive membranes are polymer membranes that change confirmation in response to an external stimulus. For this work, the focus will be on designing magnetically responsive membranes, specifically a membrane that responds to an external magnetic field. In order to reach this aim, a solid foundation of understanding must be established and can be divided into two categories: modification of membrane surface properties and stimulus responsive membranes.

### *2.1 Modification of Membrane Surface Properties*

Stimulus responsive membranes typically involve using a stimulus responsive polymer and incorporating the polymer into a membrane. The goal is to modify the surface properties of the membrane. There are two main methods by which to modify membrane surface properties: surface grafting or membrane processing. The two methods of changing membrane surface properties have both advantages and disadvantages. Membrane processing changes the surface properties of the membrane by casting the membrane with a polymer with special characteristics. In this method, changes are not localized to the membrane surface, but are distributed through the bulk of the material. There are multiple ways to cast membranes, among them are precipitation of a polymer from a non-solvent, solvent evaporation, precipitation by absorption of the non-solvent into another phase, and precipitation by cooling.<sup>6</sup> This would be advantageous when attempting to confer responses to the entirety of the membrane and has been performed with both temperature responsive and pH responsive polymers.<sup>13-17</sup> However, due to changes in

the bulk material, it is more difficult to maintain desirable bulk properties such as permeability, charge, mechanical, and chemical integrity.<sup>11</sup>

Surface grafting of polymers can be done using physical attachment or chemical attachment. Of the two ways, chemical attachment is more permanent and is less likely to degrade with time, which is especially important in UF biomedical processes because any leaching of polymer into the product stream can have negative effects on the final product. While there are instances of physical attachment of pH responsive polymers, chemical attachment of polymers make up the majority of the work in responsive membranes.<sup>11</sup>

Chemical reactions used to graft polymers to the membrane surface fall into two categories: grafting polymers using existing grafting initiation sites on the native membrane polymer (hydroxyl, amino, or carboxylic groups) and grafting polymers on initiation sites that were added to the native membrane polymer. Surface modification using existing initiation sites is an ideal case for grafting polymers onto membrane surfaces, but native initiation sites may be slow to react or low in concentration.<sup>6</sup> Thus, addition of initiation sites to polymer membranes is employed to add more reactive initiator sites and a higher concentration of sites.

Addition of initiator sites to membranes can occur chemically or physically. Chemical addition of initiator sites, usually involves addition of an initiator molecule that has a greater ability to react and start polymerization, some common initiators are 2-bromo-isobutyl bromide (BiB), degradation of peroxide solutions to create radical initiator sites, and benzophenone, which creates radical initiator sites when exposed to UV radiation.<sup>6</sup> Physical addition of initiator sites involves degradation of the polymer to create radical sites by high energy radiation, plasma, and UV irradiation.<sup>6</sup> However, degradation of the polymer membrane must be carefully controlled to avoid complete loss of bulk membrane properties due to aggressive polymer

degradation. Kochkodan et al. summarizes surface modification research via graft polymerization using UV degradation and UV-assisted initiation with benzophenone.<sup>18</sup> The paper describes the addition of a variety of polymer chains and presents methods to graft polymers: a “grafting to” mechanic and a “grafting from” mechanic.

Grafting polymers using a grafting to method involves the attachment of preformed polymer chains to the surface of the membrane. In this method, the polymer will be synthesized with a chemically reactive group that can chemically attach to a membrane initiator site. The advantage of this method is that the polymer chain length can be easily controlled and the polydispersity is very low.<sup>11</sup> However, it is difficult to achieve high grafting densities using this method due to steric hindrance from other grafted polymers.

Grafting polymers using the grafting from methods involves growing polymer chains from the membrane surface. Typically, this method uses radical polymerization reactions and start at radical sites on the membrane surface.<sup>6</sup> This method yields higher membrane chain density, but suffers from termination effects that result in higher polydispersity in the polymer chains. Ultimately, determining the optimal grafting method is based on each individual case, the desired outcome (i.e. fouling resistance, gated membranes, etc.), and the attached polymer.

Atom transfer radical polymerization (ATRP) is a grafting from technique that will be used in this thesis for membrane modification. ATRP, like other polymerization techniques creates a radical to grow polymers. Unlike other polymerization techniques (UV initiated polymerization and plasma initiated polymerization), ATRP provides a more controlled polymerization reaction that enables controlled growth as a function of polymerization time.<sup>19</sup> This is especially important when grafting polymers because controlled polymerization rates allow more even growth of the chains and lower termination events. In traditional radical

polymerization methods, the large concentration of radical chains leads to premature termination events. However, a low concentration of radicals would facilitate high MW polymers and high polydispersities. ATRP overcomes traditional radical polymerization problems with the reversible deactivation of growing radical polymer chains. The halogen on a dormant alkyl halide will covalently bond with a metal complex. This will create a radical on the alkyl in a traditional activation step. The radical carbon species will react with a monomer in solution in a typical propagation step. Ultimately, a high concentration of radicals will result in the deactivation of the radical chains via the metal complex to produce dormant alkyl halide species. The controlled growth comes from this equilibrium between radical chains and dormant chains.<sup>20</sup> For example, copper(I) chloride would promote polymerization and create more radical chains, while the lower oxidation state compound copper(II) chloride would reduce radical chains and slow down polymerization.<sup>21</sup> In addition, a chemical ligand is needed in ATRP reactions to stabilize the transition state of the halide compound. Matyjaszewski et al. provides an excellent review of this technique and Figure 2 gives a schematic representation of the chemical reaction.<sup>19</sup>

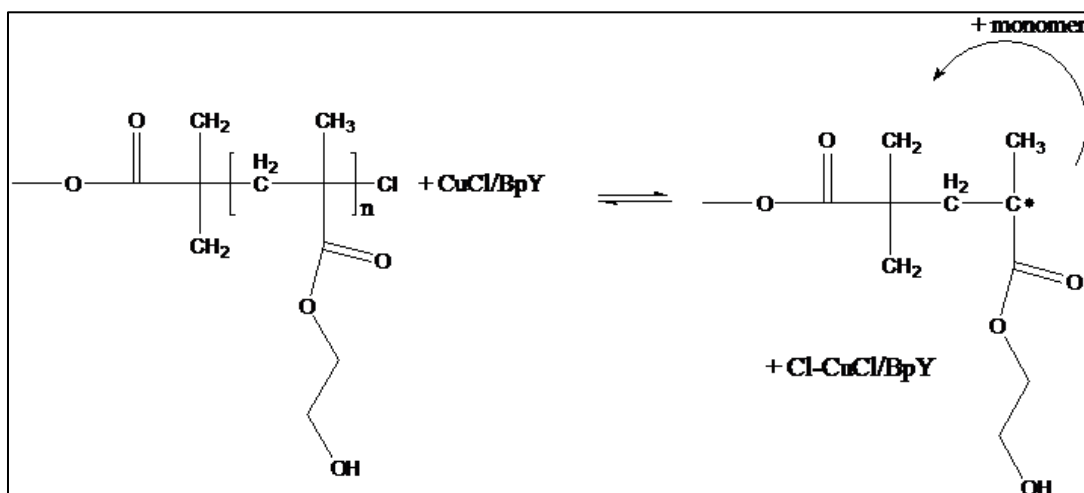


Figure 2: Schematic Representation of the ATRP reaction.

## 2.2 Stimulus Responsive Membranes

Various monomer materials have been used to modify membranes, which include but are not limited to: N-vinyl-2-pyrrolidone (NVP), N-vinylformamide (NVF), 2-hydroxyethyl methacrylate (HEMA), poly(ethylene glycol (PEG), poly(ethylene glycol) methacrylate (PEGMA), 2,4-phenylenediamine (PDA), ethylene diamine (EDA), and poly(dimethylsilohexane).<sup>18</sup> In addition to these traditional polymers, there have also been widespread investigations into stimulus responsive polymers. Stimulus responsive polymers are chains that change properties based off of external stimuli; a few select examples are listed in Table 1. Attachment of stimulus-responsive polymers to membranes creates stimulus-responsive membranes. Stimulus responsive membranes are of particular interest when reducing fouling because they can be designed to be self-cleaning based solely on external stimuli properties.<sup>11</sup>

Table 1: Examples of stimulus responsive polymers that lists the external stimulus, the membrane matrix material, and modification method.

Responsive Polymer	Stimulus	Membrane Matrix Material	Modification Method
Poly(N-isopropylacrylamide)	Temperature	Polyethylene terephthalate	Pore-Filled Crosslinking <sup>22</sup>
Poly(Acrylic Acid)	pH	Polyacrylonitrile (PAN)	Membrane Synthesis <sup>23</sup>
Poly (N,N-dimethylaminoethyl methacrylate (PDMAEMA)	pH and Temperature	Polystyrene (PS)	Membrane Synthesis <sup>14</sup>
Poly(methylacrylic acid)	pH	Poly(ethylene)	UV Grafting <sup>24</sup>
Poly(spiropyran-containing methacrylate)	Photo-responsive	Poly(tetrafluoroethylene)	Surface Modification (grafting from) <sup>25</sup>



It is important to note that special consideration must be given to the chain density, chain length, and polydispersity index; as all of these factors may result in lack of observable response. A chain density that is too high or too low may result in lack of observable response due to steric hindrance and sparse responses, respectively.<sup>11</sup> Polymer chain lengths that are too long or too short may result in no response due to physical constraints or minimized macro effect.<sup>11</sup> A high polydispersity index may cause a non-uniform response because of a lack of a homogeneous response. Thus, it is vital that the polymerization method be controlled to ensure reproducibility; a controlled polymerization method such as ATRP.

### *2.3 Temperature Responsive Membranes*

Membranes with temperature responsive characteristics are typically created by grafting poly(N-isopropylacrylamide) (PNIPAAm) onto the surface. PNIPAAm is a polymer that has a lower critical solution temperature (LCST) at 32 °C. Below the LCST, PNIPAAm hydrates and is soluble in aqueous solution; above the LCST PNIPAAm precipitates out of solution. When PNIPAAm chains are grafted onto membrane surfaces they cannot precipitate or dissolve like in solution, instead they will hydrate and expand below the LCST and collapse into globular structure above the LCST. This provides some novel effects when exposed to different temperature solutions and under moderate chain density can provide a layer on the membrane surface that changes topography based on the temperature of the solution.<sup>26</sup> By taking advantage of the change in surface topography, investigators found that PNIPAAm modified membranes had reduced fouling and greater cleaning efficiency characteristics.<sup>27-29</sup> The change in physical characteristic of the polymer was also investigated as a way to tune the permeability of the membrane modifying the pores with PNIPAAm.<sup>22,30,31</sup> However, it is noted that temperature

responsive membranes suffer from having to change the characteristics of the bulk feed, which may damage desirable products and lead to greater operating costs.<sup>11</sup>

#### *2.4 pH Responsive Membranes*

Polymers that are pH responsive exhibit different characteristics when exposed to different ionic solutions above and below their pKa. When attached to membranes, the polymers will either be in an expanded or collapsed conformation due to electric-repulsion and hydration within the chain. Some of the typical pH responsive polymers include carboxyl and pyridine functional groups, such as poly(acrylic acid) (PAA), poly(methacrylic acid) (PMAA), and methyl acrylate.<sup>32</sup> Using the pH responsive collapsed and hydrated states of these polymers, investigators have studied the effects of blending these polymers into membrane casting solutions on filtration and fouling resistance.<sup>15–17,23</sup> In addition, surface modification of existing membranes was also investigated as application for tunable membrane permeability.<sup>33,34</sup> There were also attempts to create a double stimulus-responsive membrane that incorporated both temperature and pH responsive properties.<sup>14</sup> However, similar to temperature responsive membranes, the need to alter the feed characteristics poses problems to the end product and additional costs for adjusting the pH of the solution.

#### *2.5 Magnetic Responsive Membranes*

Magnetically responsive membranes are a new area of stimulus responsive membranes and unlike temperature and pH responsive membranes the stimulus is external to the membrane unit operation. The main focus for imparting magnetic response in membranes is to incorporate Fe<sub>3</sub>O<sub>4</sub> superparamagnetic NP into the membranes.

Superparamagnetic NP's have, by definition, a single magnetic domain. In the presence of an external magnetic field the single magnetic domain will align itself with the external

magnetic field. Upon removal of the external magnetic field, the single magnetic domain of the NP will randomly orient itself by two competing mechanisms: Néel relaxation and Brownian relaxation. In Néel relaxation, the internal magnetic spin of the domain will change and the time it takes is called the Néel relaxation time. For Brownian relaxation, the NP will physically move to randomly orient itself with no internal change in the magnetic spin of the domain and the time it takes is called the Brownian relaxation time. In the two mechanisms, Néel relaxation is exponentially proportional to the magnetic volume of the NP and Brownian relaxation is linearly proportional to the hydrodynamic volume.<sup>35</sup> In other words, Néel relaxation will be the dominating mechanism in larger NP and Brownian relaxation will be the dominating mechanism in much smaller NP. The Néel relaxation and the Brownian relaxation can also be used to describe the alignment with an external magnetic field. In the case of an oscillating magnetic field, the frequency of oscillating will determine which mechanism dominates; for high frequency ( $> 200$  kHz), Néel relaxation, and for low frequency ( $< 25$  Hz), Brownian relaxation. By determining the dominating mechanism via NP size and oscillating frequency, investigators have observed NP heating, where the Néel relaxation mechanism dominates, and NP movement, where the Brownian relaxation mechanism dominates.<sup>12,36-38</sup>

In one study, investigators coupled the heating effect of the NP in an oscillating magnetic field with the temperature responsive polymer PNIPAAm.<sup>39</sup> Both the NP and PNIPAAm were functionalized on the surface of polyethylene terephthalate (PET) MF membranes and in the membrane pores. Upon heating of the NP in the presence of a high frequency oscillating magnetic field, PNIPAAm polymer chains took on a collapsed conformation, which created larger pores and greater permeability, as tested by water flux experiments.<sup>39</sup> Surface modification inside the pores was also used in a similar study that resulted in the possibility of

tunable pore diameters. Himstedt et al. modified MF membranes with NP capped poly(HEMA).<sup>40</sup> In the presence of both a static horizontal and vertical magnetic field, permeability of the membrane decreased. The findings were attributed to expansion and contraction of the polymers inside the pores due to movement of magnetic NP's attached to the end of the polymer chain.<sup>40</sup> In another study, surface modification was localized to the membrane surface by using polyamide composite NF membranes, where the pore size of the membrane was much smaller than the NP.<sup>12</sup> In the presence of a switching magnetic field, it was shown to produce flow near the membrane surface. This was applied during filtration and modified membranes showed improved performance. Himstedt et al. hypothesized that the membrane surface flow disrupted concentration polarization, which enhanced flux for the modified membranes.<sup>12</sup> This phenomenon was further investigated by changing the density of the chains and thereby the concentration of NP on the membrane surface.<sup>41</sup> While the same increased salt rejection and permeate flux was observed in both high and low chain density modified membranes, the high chain density modified membranes exhibited a much stronger effect.<sup>41</sup>

As stated previously, the advantage of magnetically responsive membranes over other responsive membranes is an external stimulus from the membrane unit operation. In all studies, the presence of an external magnetic field allowed localized changes in the membrane; heating, permeability, or surface mixing. In the case of heating and permeability, these phenomena were observed in the case of membrane processing and surface modification. In the case of surface mixing, this phenomenon was only observed with surface modification. This is logical given the limited mobility of NP when encased in a polymer matrix. However, surface mixing was only ever applied to NF and MF membranes. Surface modification of UF membranes has not been

attempted and given the significant issues of UF processes and concentration polarization this is an area of much needed research. The work in this thesis attempts to bridge the gap between NF and MF by designing magnetically responsive, surface modified UF membranes.

### 3. Experimental

#### 3.1 Membrane Modification

The membranes used in this work were 100 kDa MWCO RC membranes (Sartorius; Göttingen, Germany). The chemicals used for modification were high purity grade acetonitrile (Fischer Scientific; Fair Lawn, NJ), high purity grade methanol (Fischer Scientific; Fair Lawn, NJ), 2-bromo-isobutyl bromide (Sigma Aldrich; St. Louis, MO), triethylamine (TEA) (Sigma Aldrich; St. Louis, MO), copper (I) chloride (Sigma-Aldrich; St. Louis, MO), copper (II) chloride (Sigma-Aldrich; St. Louis, MO), 2,2'-bipyridine (BpY) (Sigma Aldrich; St. Louis, MO), HEMA (Fischer Scientific; Fair Lawn, NJ), copper (I) bromide (Sigma-Aldrich; St. Louis, MO), copper (II) bromide (Sigma-Aldrich; St. Louis, MO), N,N',N'',N''' - pentamethyldiethylenetriamine, 1,2 epoxy-5-hexene (Sigma Aldrich; St. Louis, MO), and amine coated Fe<sub>3</sub>O<sub>4</sub> NP (Ocean Nanotech; San Diego, CA).

In order to attach the NP capped polymer to the membrane surface, an ATRP modified method was developed as illustrated in Figure 3. First, 25 mm diameter membranes were punched out of an 8 x 11 inch sheet. The membranes were rinsed in methanol for 20 minutes in order to remove any chemical preservatives added during the manufacturing process. This was followed by two de-ionized (DI) water rinses for 15 minutes to remove any remaining methanol.

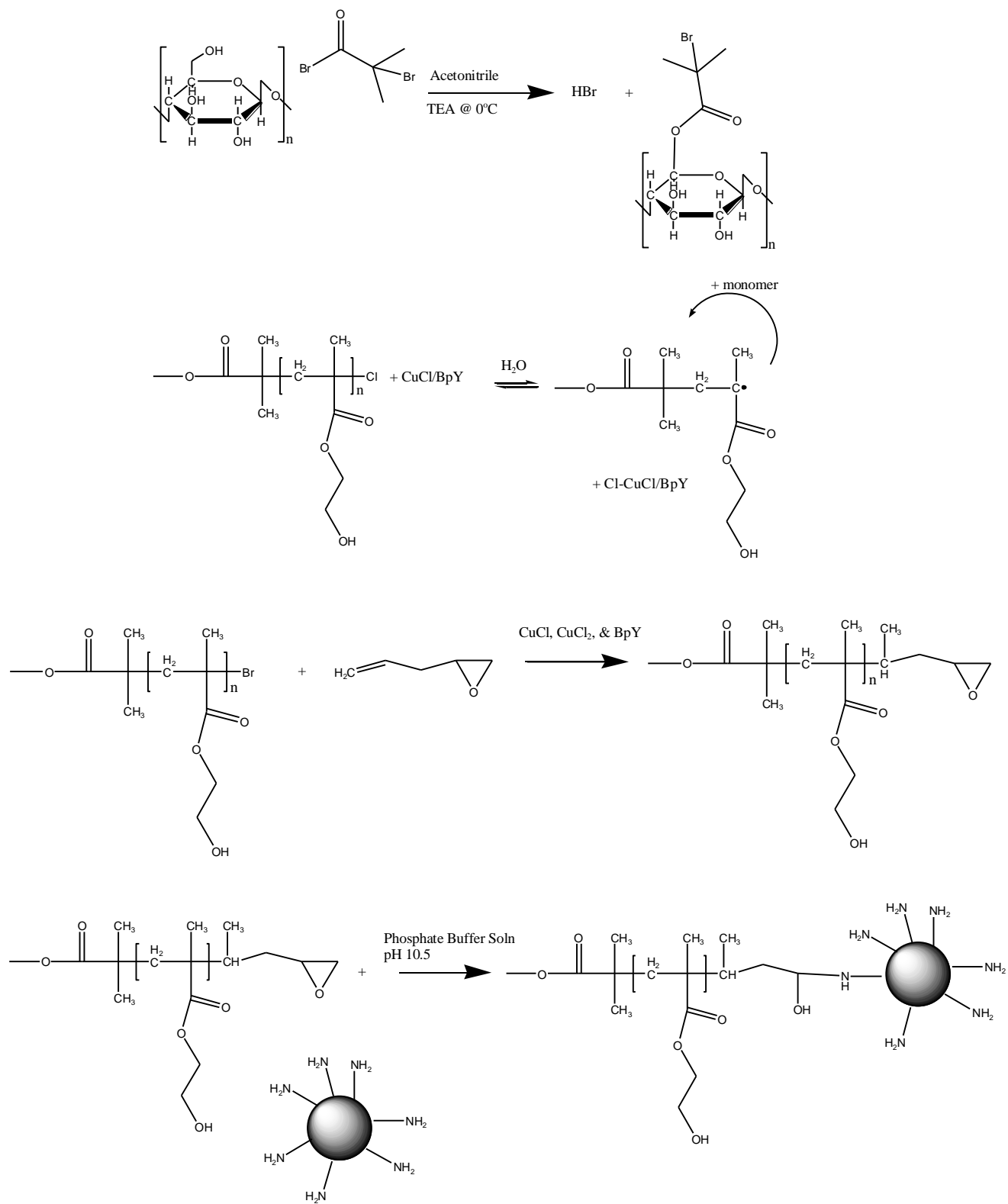


Figure 3: Diagram of chemistry used to modify UF RC membranes.

Once rinsed, the membranes were placed in pure acetonitrile and allowed to equilibrate for 10 minutes. Afterwards, the membranes were placed in the initiator immobilization solution at 0°C, which consisted of 1 mM of TEA and 1 mM of BiB in an acetonitrile solution. The membranes were kept in the initiator immobilization solution on a shaker and allowed to react for 5 minutes. Membranes were then removed from the solution and placed in a solution of pure acetonitrile and rinsed for 30 minutes. The acetonitrile rinse was followed by one, 15 minute rinse in methanol and two, 15 minute rinses in DI water. Membranes were then placed in DI water on a shaker overnight to remove any residual solvent.

Next the initiator immobilized membranes were placed in an ATRP solution and allowed to react at room temperature (27°C) under an argon environment. The ATRP solution consisted of 100 mM HEMA, 0.5 mM of copper (I) chloride (Cu(I)Cl), 0.1 mM of copper (II) chloride (Cu(II)Cl), and 1.5 mM of BpY. Membranes were allowed to react for 30 minutes and 1 hour. The reaction was ended by immersing the polymer modified membranes in a quenching solution for at least 30 minutes. The quenching solution consisted of 625 µL N,N',N'',N''' – pentamethyldiethylenetriamine and 250 mg of copper(II) bromide dissolved in 50 mL of a 50:50 by volume mixture of methanol and water. Following the quenching step the membranes were rinsed with DI water and washed twice with DI water for 30 minutes, a 50:50 by volume mixture of methanol and water, and finally placed in DI water overnight.

After growing the main poly(HEMA) chain from the membrane, the NP was attached via a two-step process. The first involved a monomer addition reaction via ATRP as adapted from Coessens et al.<sup>42</sup> The membranes were immersed in an ATRP solution consisting of 28.8 mM BpY, 5.58 mM of Cu(I)Br, and 17.7 mM of 1,2-epoxy-5-hexene dissolved in a 50:50 by volume mixture of methanol and water. Membranes were allowed to react in an Argon gas environment



at 50°C for 24 hours. The long reaction time was to ensure addition of 1,2-epoxy-5-hexene to the p(HEMA) chain. After 24 hours, the membranes were rinsed with DI water and washed in DI water for 15 minutes. Next the membranes were allowed to equilibrate in a phosphate buffer solution (PBS), pH 10, for 30 minutes. A maximum of 2 membranes were then immersed in a 20 mL PBS, pH 10, with 15  $\mu$ L of the NP solution from the manufacturer. Membranes were allowed to react at room temperature for 48 hours in covered containers. After 48 hours, the membranes were rinsed and then washed with DI water overnight. A detailed step by step document can be found in the appendices under “Modification of Regenerated Cellulose Protocol”.

### *3.2 Surface Characterization*

Three surface characterization methods were employed to determine successful attachment of NPs: X-Ray Photospectroscopy (XPS), atomic force microscopy (AFM), and scanning electron microscopy (SEM). Prior to measurement all membrane samples were allowed to dry to remove any water.

XPS scans were run at a 45° projection angle and analyzer pass energy of 23.5 eV (Fayetteville, AR). A general survey scan (interval: 1 eV) was taken of the unmodified membrane, the ATRP modified membrane, and the final NP modified membrane from 100 to 900 eV. In addition, high definition scans (intervals: 0.1 eV) were taken of the carbon region (250 eV to 300 eV), the iron region (700 eV to 800 eV), and the nitrogen region (390 to 410 eV) to determine the surface chemistry at each step of the modification process.

AFM images were obtained with Bruker Icon Atomic Force Microscopy (Bruker Corporation; Billerica, MA). Measurements were taken at room temperature using the

ScanAsyst in Air probe (Bruker Corporation; Billerica, MA). Continuous scans with an area of one  $\mu\text{m}^2$  were taken of all membrane samples.

SEM images were obtained with the FEI Nova Nanolab 200 Duo – Beam Workstation (Hillsboro, OR). Images were taken at 25,000x and 50,000x magnification.

### *3.3 Flux Measurements*

Two separate flux measurements were made of the membrane; DI water flux measurements and bovine serum albumin (BSA) protein filtration measurements. DI water flux measurements were taken as a baseline to determine the effect of membrane modification and the BSA protein filtration measurements were used to determine modified membrane proof of concept. Both flux measurements were performed at room temperature in dead end mode in Amicon (Millipore; Darmstadt, Germany) flux modules for UF and MF membranes.

For the DI water flux measurements the membranes were compressed at 29 psi for 1 hour prior to measurements. The flux of modified and unmodified membranes were tested for 1 hour with no stirring and then for 1 hour under the presence of an oscillating magnetic field (.93 A and 20 Hz) at 14.5 psi. The permeate was collected and measured at 1 minute intervals and used to calculate the flux through the membrane samples.

The BSA protein filtration measurements were performed at 6.2 psig. This pressure was chosen to reduce irreversible fouling effects and build-up of a cake layer, since the focus of the work was to look at suppression of concentration polarization. The feed solution was a 0.1 g/L BSA solution in a 10 mM sodium phosphate buffer solution of pH 5. The pH of the buffer solution was picked to be as close to the isoelectric point of BSA (pI 4.7) as possible without exceeding the pH stability range of the  $\text{Fe}_3\text{O}_4$  NP's (pH 5 – 10). Permeate weight was collected and weighed at 5 minute intervals to calculate the membrane flux. During the course of the

measurement an oscillating magnetic field (.93 A and 20 Hz) was run for 1 hour and then turned off. Samples of the permeate were also taken to determine how the membrane rejection changed during the course of the flux experiment. A detailed protocol for the BSA protein filtration experiments may be found in appendices under “BSA Filtration Protocol”.

### *3.4 Dextran Rejection*

A Showa Denko SB-G guard column (Showa Denko; Tokyo, Japan) was used to protect the gel permeation chromatography (GPC) column from Showa Denko SB-806M HQ (Showa Denko; Tokyo, Japan), which was used for analyzing the dextran samples. The eluent solution for the high performance liquid chromatography (HPLC) analysis was a 50 mM  $\text{KH}_2\text{PO}_4$  buffer solution adjusted to pH 7 by a 50 mM NaOH solution. The HPLC analysis was run at a flow rate of .4 mL/min and a temperature of 35°C. Individual dextran fractions were dissolved in the same buffer solution as the eluent solution and used to determine elution times and develop a calibration curve of elution time vs. molecular weight (MW). Interference from the buffer solution was detected and removed by dissolving dextran standards in a buffer solution with DI water dilution of 5.5% by volume. The dextran fractions were then combined at concentrations listed in Table 2 as adapted from Zydney et al.<sup>43</sup>

Table 2: Dextran fraction concentrations as adapted from Zydney et al.<sup>43</sup>

Dextran Fraction	Concentration (g/L)
T1	.74
T4	1.22
T10	.54
T40	.74
T70	.34
T500	.27
T2000	3.65

These concentrations were found by Zydney et al. to provide a wide swath of dextran sizes and improve accuracy of dextran rejection experiments.<sup>43</sup>

Dextran rejection studies were run with the combined dextran fraction solution, challenge solution. The challenge solution (10 mL) was loaded into a dead-end filtration module and pumped through the membrane at 0.4 mL/min on total recycle for 1 hour. To decrease the effect of concentration polarization, the challenge solution was stirred at a rate of 300 rpm. After the 1 hour equilibration period, the permeate solution was allowed to run without recycle and samples of the permeate and the retentate were collected immediately after equilibration and after 30 minutes. This was completed for modified membranes with NP's and modified membranes with just the poly(HEMA) polymer attached.

## 4. Results

### 4.1 Surface Characterization

High definition XPS scans were taken of the control RC membrane, the poly(HEMA) modified membrane, and the NP modified membrane. One scan was in the carbon region (250 eV to 300 eV) [Figure 4] and shows three prominent peaks: C-H peak (283 eV), C-OH peak (285 eV), and an C=O peak (287 eV). From Figure 4, there are changes in the carbon surface chemistry at each step of the modification process. In addition, the C-H peak increases after attachment of poly(HEMA). There is also a decrease in the C=O peak relative to the C-OH peak when comparing the monomer attached modified membrane and the ATRP modified membrane. These changes are the result of successful attachment of poly(HEMA) and the addition of C-H bonds from the HEMA monomer structure. The decrease in C=O peak can be associated with interference from the epoxide monomer structure. Figure 5 shows the high definition XPS scan of the iron magnetite region (250 eV to 300 eV). As apparent from Figure 5, there is a clear peak at 710 eV and a slight peak at 720 eV. High definition XPS scans of the nitrogen region (390 to 410 eV) [Figure 6], reveal a distinct nitrogen peak at 398 eV for NP modified membranes. This peak is a result of the amine coatings on the NPs and the result of chemical bonding of the monomer and the amine groups on the NPs.

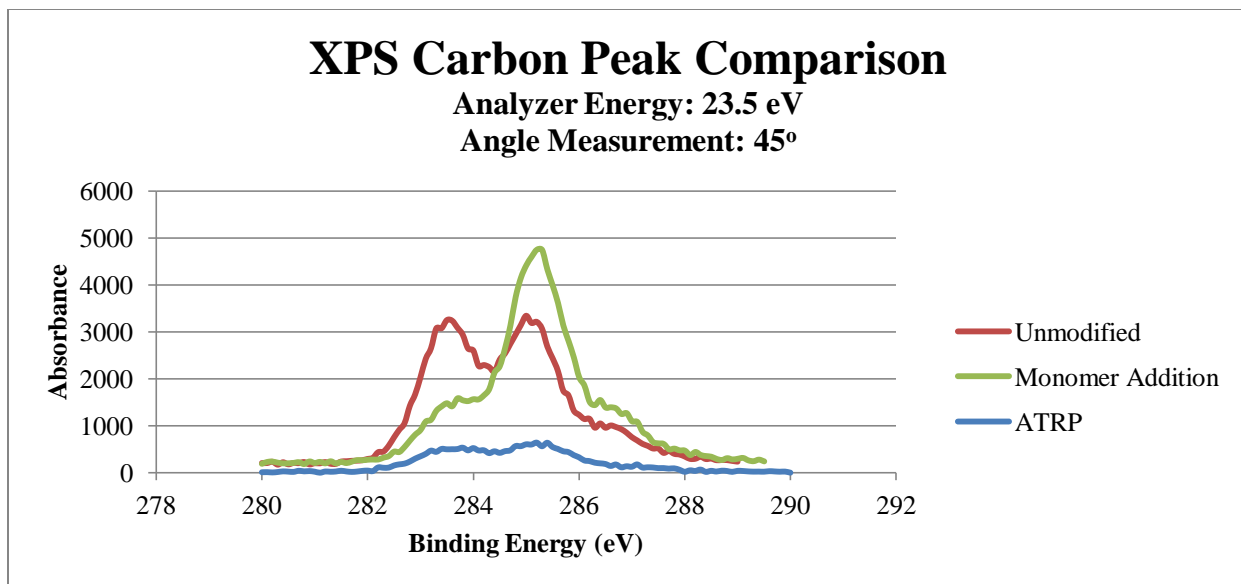


Figure 4: XPS carbon peak diagrams for the unmodified membrane, after ATRP polymerization, and after the monomer addition reaction.

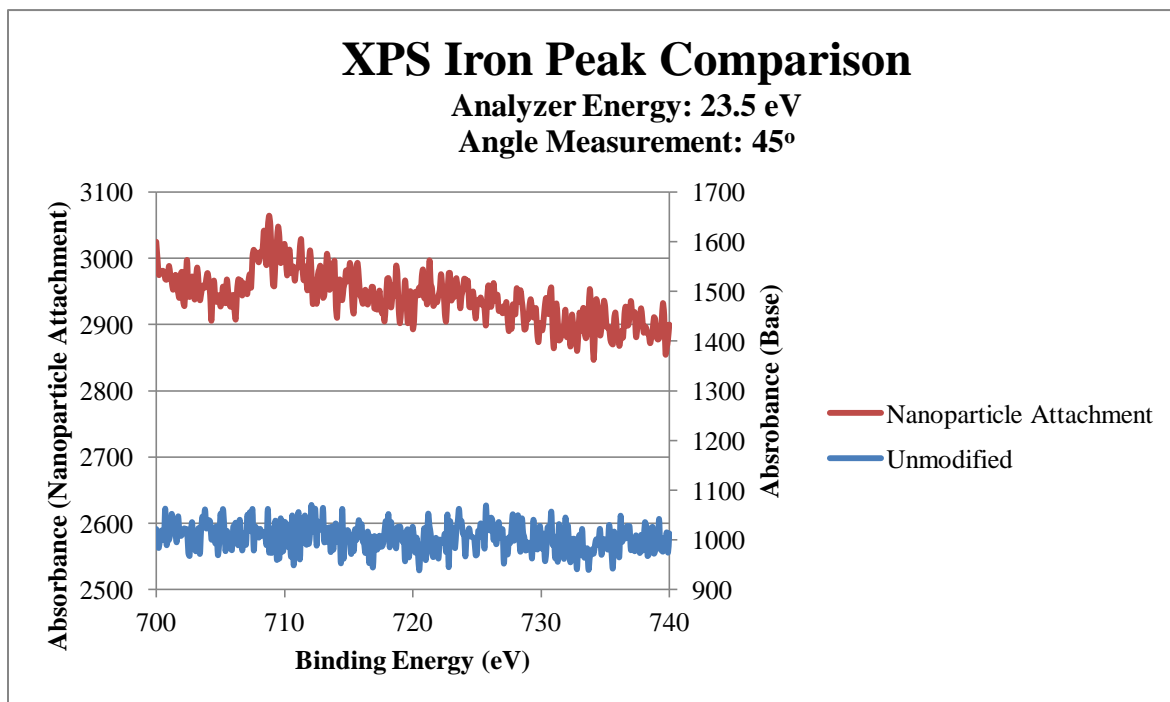


Figure 5: XPS iron peak diagrams for the unmodified membrane and NP modified membrane

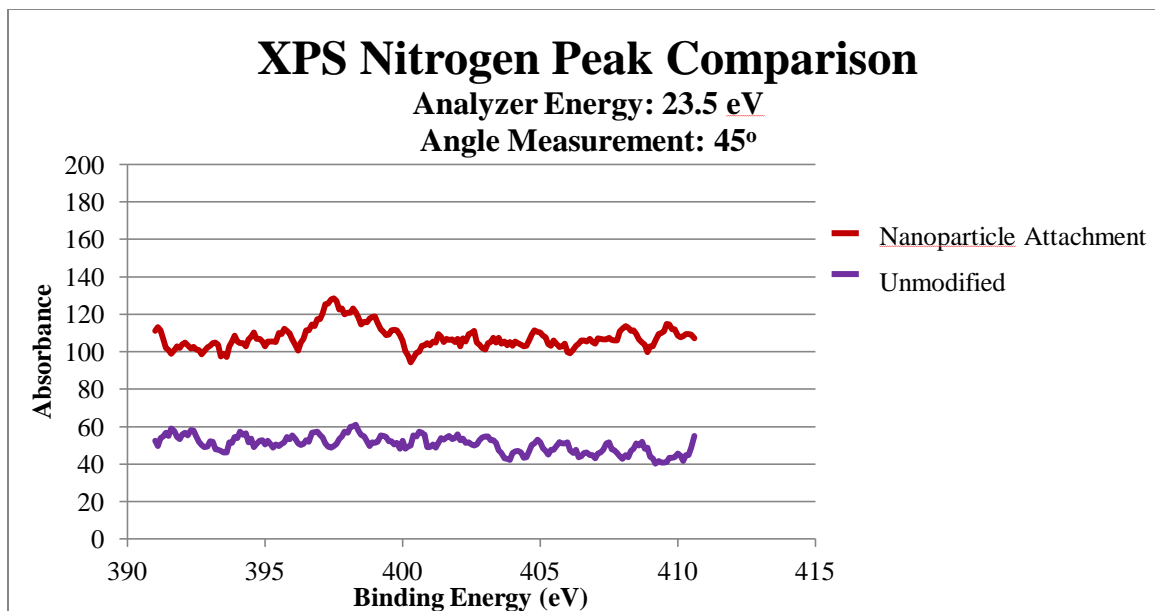


Figure 6: XPS nitrogen peak diagrams for the unmodified membrane and the NP modified membrane.

AFM was another supporting technique to confirm successful modification of the RC membranes. Three images were taken of the control RC membrane, the poly(HEMA) modified membrane, and the NP modified membrane. [Figure 7] After the poly(HEMA) modification, it is clear that there is a change in surface topography from the control RC membrane. The NP modified membrane shows a different topography to the poly(HEMA) modified membrane and contains circular objects, roughly 25 nm in diameter

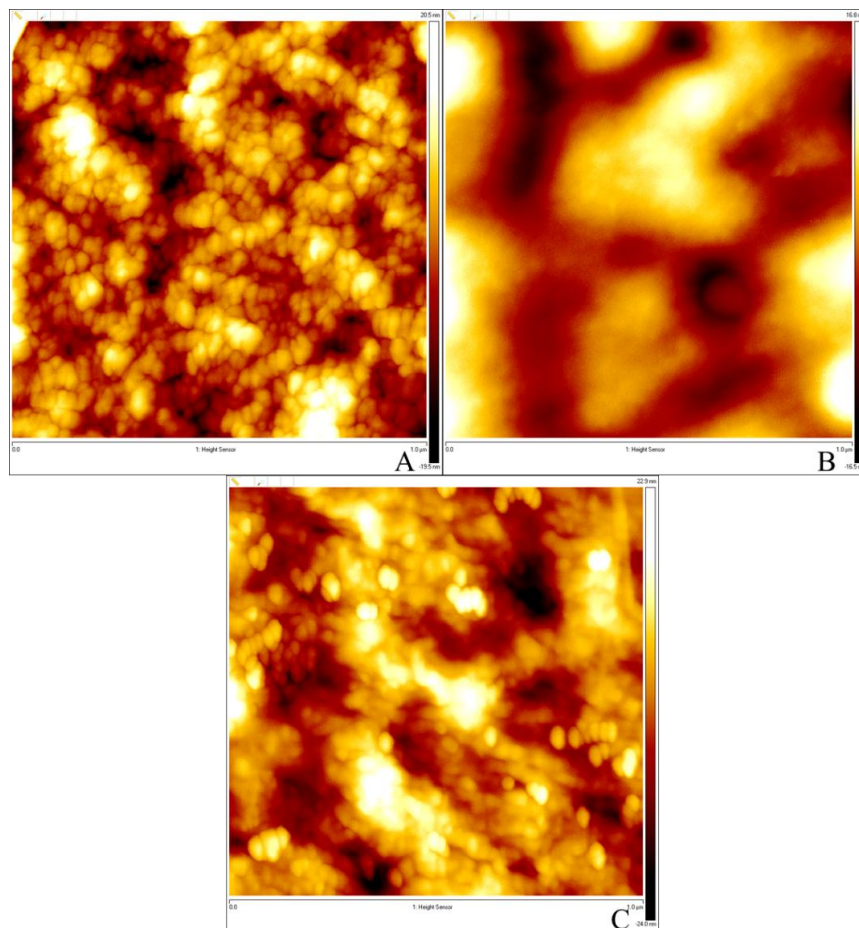


Figure 7: AFM images of unmodified membrane (A), poly(HEMA) modified membrane (B), and the NP modified membrane (C).

SEM was another visual surface characterization method used to determine successful modification of the membrane surface. Two images of different magnification were taken of an unmodified membrane surface and an NP modified membrane surface. Differences between the unmodified membrane surface and the NP modified membranes surface include a less cracked surface and spherical objects with diameters of about 25 nm range uniformly covering the membrane surface. From the visual images at both magnifications, the spherical objects exhibit nanoparticle characteristics.



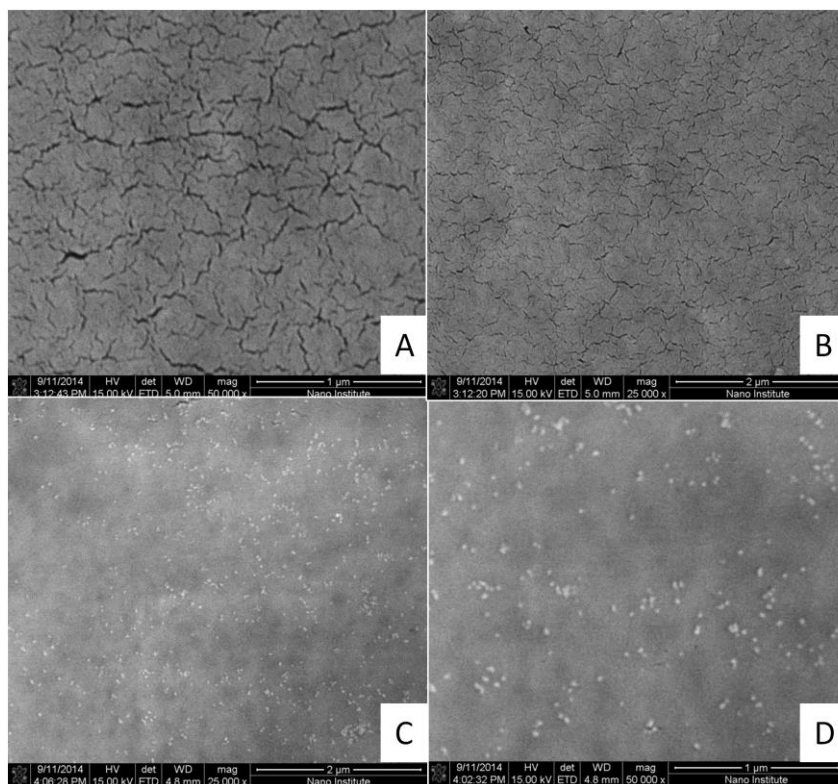


Figure 8: SEM images of the unmodified membrane surface at 25,000x and 50,000x (A and B) and the nanoparticle modified surface at 25,000x and 50,000x (C and D).

#### 4.2 Flux Measurements

DI water flux was measured as a baseline comparison and to track the membrane modification process. During the course of the modification DI water flux measurements were taken of the unmodified RC membrane, the ATRP poly(HEMA) modified membrane, and the final NP modified membrane. There were two sample sets of flux measurement data; membranes modified with ATRP for 1 hour and membranes modified with ATRP for 30 minutes. As there were no changes in membrane DI water flux during the filtration tests, the results for the measurements were compared using bar graphs that represent the average value of DI water flux for 4 membranes. Figure 9 summarizes the flux measurements for 1 hour and 30 minutes. In both cases, there is a clear drop in flux after membrane. There is little difference between the ATRP modified membranes and the final NP modified membranes. There is no

difference in flux between the 1 hr modified and the 30 minute modified membranes except for the base membrane, which is due to variation in the base membrane material.

BSA protein filtration flux measurements were performed on the unmodified membrane, ATRP poly(HEMA) modified membranes, and the final NP modified membranes. As with the DI water flux measurements there were two sample sets: membranes modified with ATRP for 1 hour and membranes modified with ATRP for 30 minutes. BSA protein filtration experiments were performed at 6.2 psi, an operating pressure just below the critical pressure for the 0.1 g/L BSA solution. The critical pressure was determined by measuring the flux as a function of operating pressure [see Figure 17 in appendices]. In order to isolate the concentration polarization effect from other fouling phenomena, filtration was run just under the critical pressure.

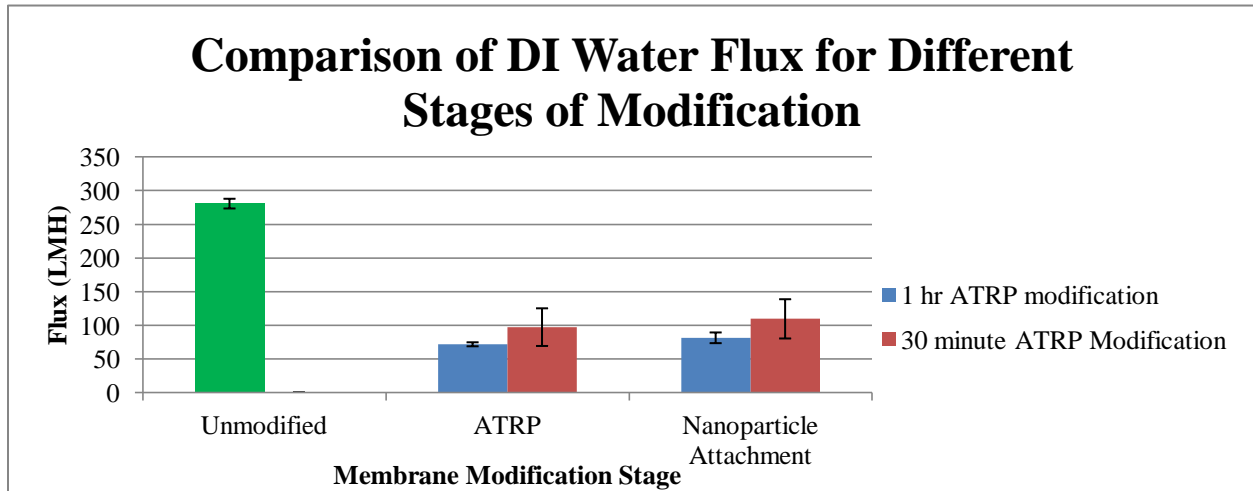


Figure 9: DI Water Flux measurements for different stages of modification. Values are an average out of 5 and the error bars represent the standard deviation.

In addition to flux measurements, rejection of the membranes were calculated from the permeate concentration at different time points and the concentration of the feed. However, due to the changing concentration of the feed this made calculating rejection for all time points difficult. In order to compensate for this obstacle, rejection data was compared after 5 mL of

permeate was filtered. Figure 10 shows the comparison of the different membranes: unmodified, 1 hour ATRP modified with NP, 1 hour ATRP modified without NP, 30 minutes ATRP modified with NP, and 30 minutes ATRP modified without NP. The conditions for each membrane are listed in Table 3. Error bars were determined by standard propagation of uncertainty throughout the calculations for rejection. There is no clear trend in the rejection data, as most differences in rejection fall within the measurement uncertainty.

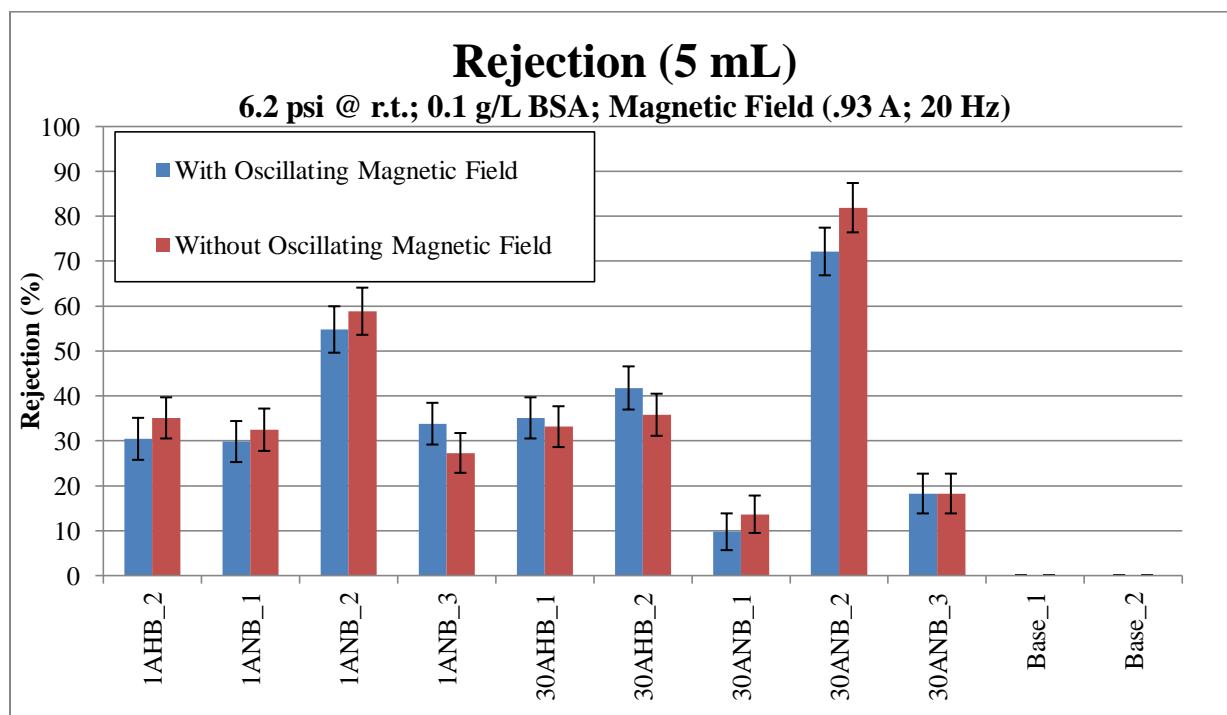


Figure 10: Rejection of BSA for different modified membranes. Error bars represent the uncertainty in the measurements as propagated through the calculations.

Table 3: Legend for membrane labels in Figure 10.

Membrane Label	ATRP Time (hr)	NP Modified (Yes/No)	Presence of Oscillating Magnetic Field (Yes/No)
1AHB_2	1	No	No
1ANB_1	1	Yes	No
1ANB_2	1	Yes	No
1ANB_3	1	Yes	No
30AHB_1	0.5	No	No
30AHB_2	0.5	No	No
30ANB_1	0.5	Yes	No
30ANB_2	0.5	Yes	No
30ANB_3	0.5	Yes	No
Base_1	0	No	No
Base_2	0	No	No

#### 4.3 Dextran Rejection

Dextran rejection was used to determine the effect of modification on the molecular weight cutoff (MWCO) of the membranes. Rejection of the challenge solution was calculated from the permeate signal and retentate signal in Figure 11. Similar graphs for membranes under different modification conditions are located in the appendices [Figure 18, Figure 19, and Figure 20]. The calibration curve was used to determine the MW from the elution time and resulted in a rejection vs. MW graph for each membrane sample; Figure 12 is an example graph. Similar graphs for membranes under different modification conditions are located in the appendices [Figure 21, Figure 22, and Figure 23]. The rejection vs. MW graph was then used to determine the MWCO, 90% rejection. Figure 13 summarizes the MWCO for the membrane samples. Each membrane condition was run in triplicate and the error bars represent the range of the membrane

samples for the respective membrane condition. Figure 14 show a sample signal from the individual dextran runs and the signal from the combined dextran sample. Figure 15 shows a comparison of the signal from the combined dextran sample and the additive signals of each individual dextran runs. The similarity in the signals is expected and confirms no interference from each individual dextran fraction. Figure 16 is the calibration curve of elution time vs. MW and was created from the individual dextran fraction samples. As expected, there is a definite drop in MWCO after modification, due to successful polymer modification. However, the decrease in dextran rejection after NP attachment was unexpected and may indicate interaction of the NP and the dextran.

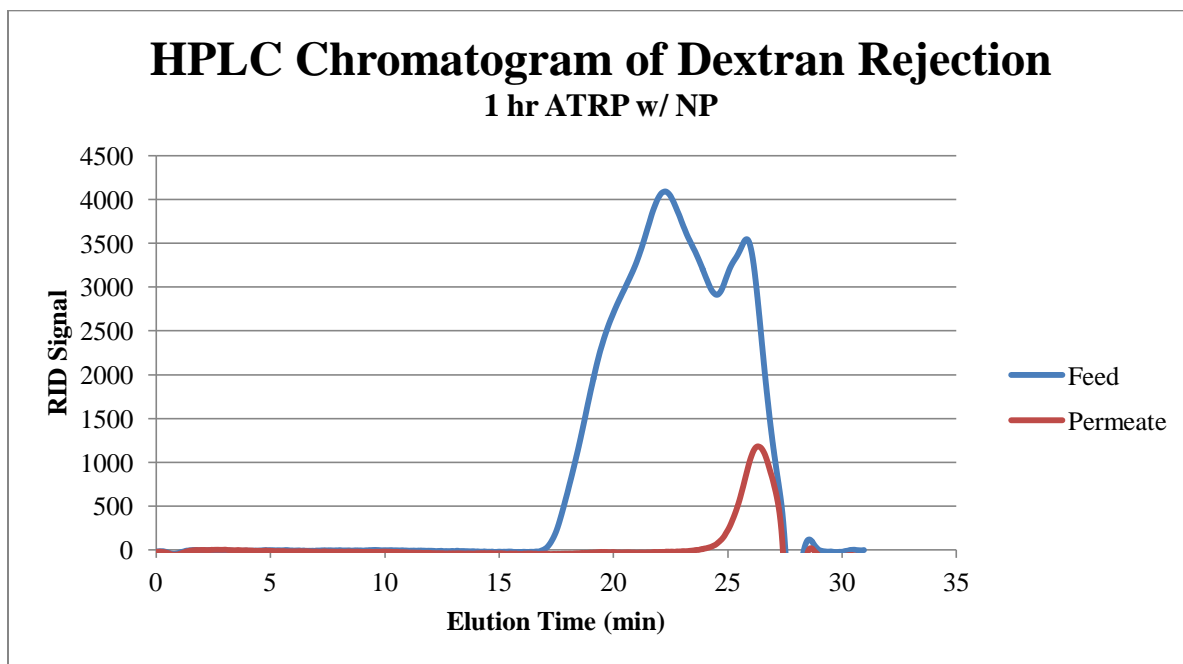


Figure 11: Dextran HPLC chromatogram for the 1 hr ATRP - NP modified membrane.

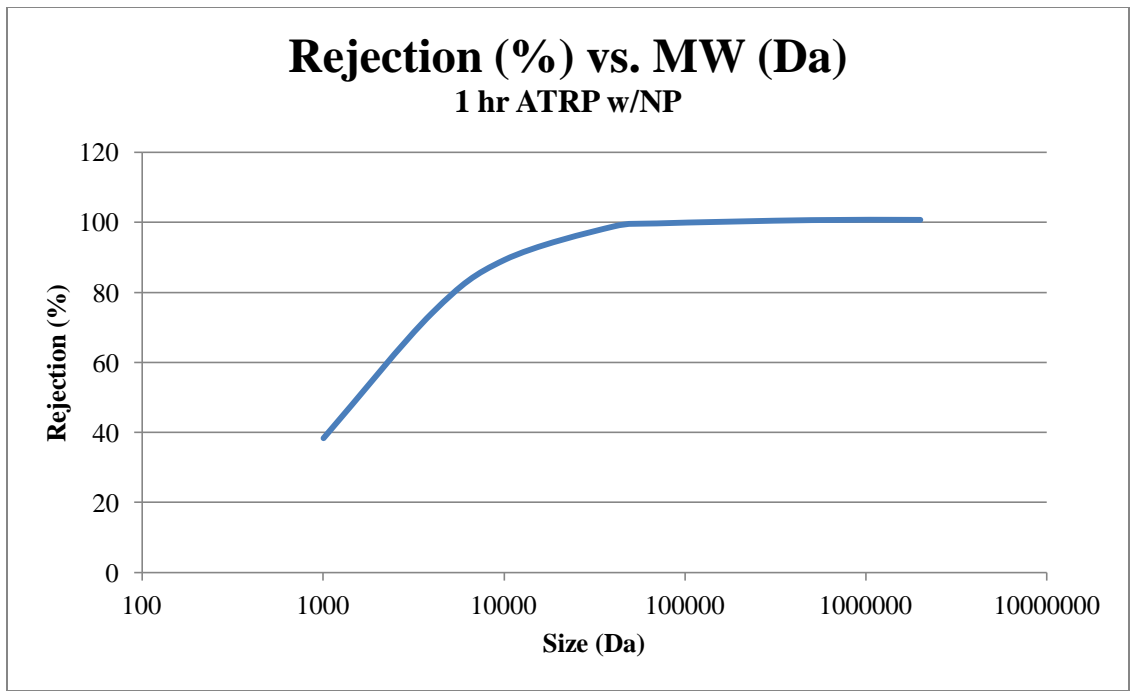


Figure 12: Rejection vs. MW curve used to determine MWCO for 1 hr ATRP - NP modified membrane.

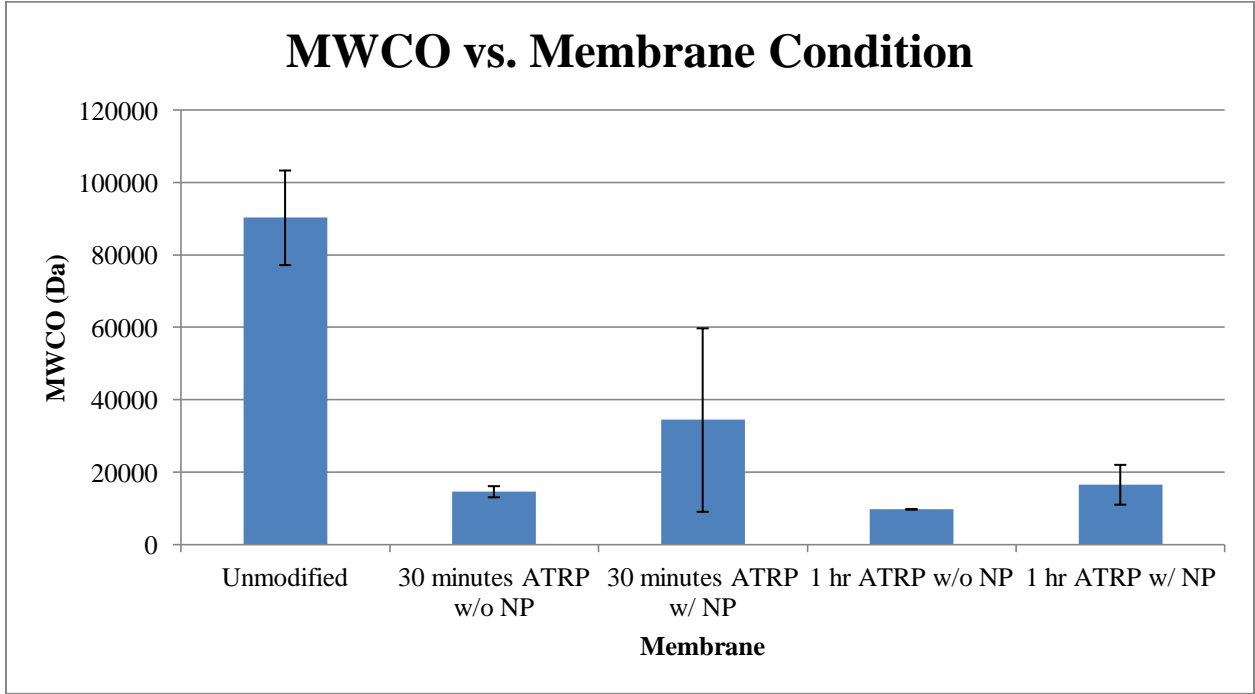


Figure 13: MWCO for modified membranes of different conditions. The values were an average of three measurements and the error bars represent the standard deviation.

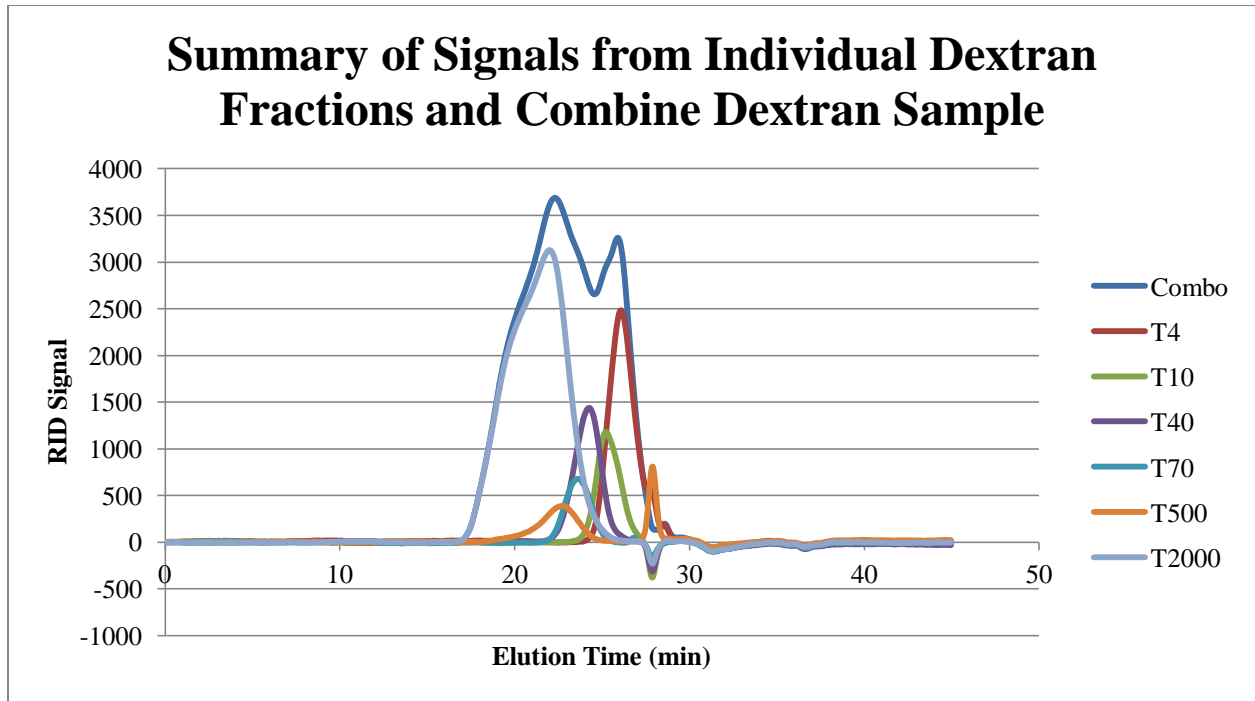


Figure 14: Summary of HPLC chromatogram signals from individual dextran fractions and the combined dextran challenge solutions.

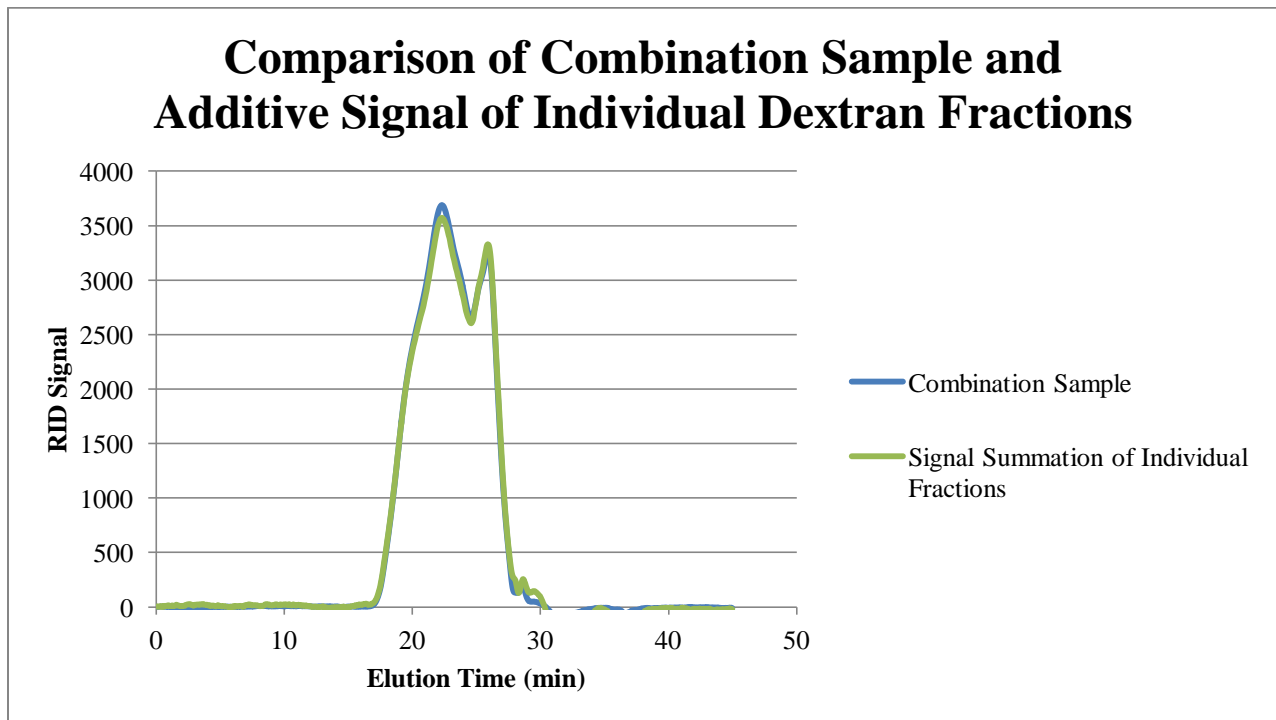


Figure 15: Comparison of dextran challenge solution and additive signal of individual dextran fractions.

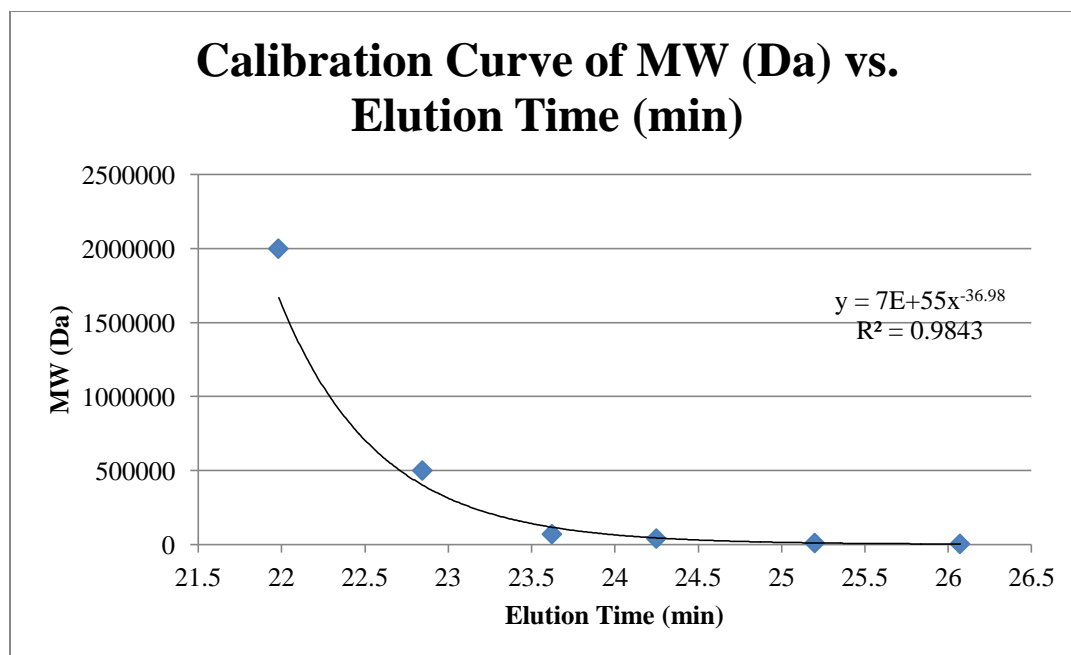


Figure 16: Calibration curve used to correlate MW (Da) of dextran with elution time (min).



## 5. Discussion

### 5.1 Surface Characterization

From the results above, it is clear that the ATRP growth of HEMA was successful. This is backed by the change in surface chemistry supported by XPS and the change in surface topography as supported by AFM. The high definition XPS scan of the carbon region, show changes in the carbon bonds during the course of the membrane modification process. In addition, there is clear evidence for successful attachment of NPs. On the XPS high definition iron peak region diagrams, there are two peaks at 710 eV and 720 eV indicating the presence of iron magnetite. In addition, XPS high definition nitrogen peak region scans show a peak at 398 eV, indicating the presence of nitrogen on the membrane surface. For the amine coated particles, this is a secondary indication of NPs present on the surface of the membrane. Finally, visual surface characterization confirmation via AFM and SEM both show 25 nm spherical objects on the modified membrane surface that are consistent with the approximate shape of the iron magnetite NPs. Thus, there is clear evidence that the attachment of NPs to the regenerated cellulose membrane was successful.

### 5.2 Flux Measurements

The DI water flux measurements show a drop in flux for ATRP modified membranes. The drop in flux is the result of successful polymer modification and an increase in membrane resistance. However, there is no statistical difference between the 1 hour ATRP modified membranes and the 30 minute ATRP modified membranes. This is not uncommon for ATRP reactions, especially at high monomer conversions. It has been found that high monomer conversions are associated with the slowing of the rate of propagation.<sup>19</sup> Slower rates of

propagation would explain why there is little difference in the DI water flux between the 1 hour ATRP modified membranes and the 30 minute ATRP modified membranes. As expected, there is little difference in DI water flux between the NP modified membranes and the ATRP modified membranes. The addition of one monomer and NP would not result in a large change in membrane resistance and thereby an insignificant change in DI water flux.

The BSA filtration studies were performed to determine the effect, if any, of an oscillating magnetic field on concentration polarization. In theory, a suppression in concentration polarization would result in an apparent decrease in rejection. However, based on the studies performed in this thesis, there is no significant change for the rejection of the modified membranes in the presence of an oscillating magnetic field. There are multiple explanations for the lack of observable effect. While proof of NP attachment is quite clear based on surface characterization, there is no clear way to determine how many polymers are attached to each NPs. Each amine coated NPs have multiple reaction sites. If more than one polymer chain is attached to each NP, this would impede free movement of the NPs in the presence of an oscillating magnetic field. Lack of movement of the NPs in the presence of an oscillating magnetic field may result in internal heating and has been documented in previous research.<sup>39</sup> Another explanation may be the result of an un-optimized chain density and length. As mentioned in the background, a chain density and length that is too high or low will result in lack of observable response.<sup>11</sup> In addition, there is large variation between the different membrane samples. The membrane samples come from different modification batches and indicate inconsistencies from batch to batch. As ATRP is highly sensitive to oxidation, a small exposure to oxygen could have a large impact on the rate of reaction and cause the large variation between batches.<sup>19</sup>

### 5.3 Dextran Rejection

The dextran rejection studies show an expected drop in MWCO after ATRP modification for both the 1 hour and the 30 minute ATRP modified membranes. The drop can be explained by a decrease in the pore size due to ATRP polymer modified membrane. The difference in MWCO from ATRP modified membranes and NP attached membrane is not significant with the 30 minute ATRP modified membranes, but shows a slight increase in the 1 hour ATRP modified membranes. This may be due to interactions of the dextran hydroxyl bonds and the amine groups on the NPs. Susanto et al. has shown that dextran interactions with membrane surface are a concern when determining MWCO with dextran.<sup>44</sup>

An interesting observation of the results is between the MWCO and the BSA rejection tests. Figure 13 shows a MWCO for all membranes of less than 60 kDa. However, Figure 10 shows the BSA rejection for all modified membranes is less than 90%, even though the MW of BSA is 66 kDa. There are a couple of explanations for this observation. From a structural standpoint, there are differences between BSA and dextran. While both macromolecules are chains, BSA is a polypeptide chain with different side chains that cause folding and a more compact physical structure. When comparing the hydrodynamic radius of the two macromolecules of similar MW, 70 kDa dextran has a calculated hydrodynamic radius of 6.49 nm, which is almost twice as big as BSA with a hydrodynamic radius of 3.48 nm.<sup>45</sup> Thereby, from a size based perspective, it makes sense that BSA would have a lower rejection percent than that of dextran. This accounts for lower MWCO measurements, but not necessarily higher BSA rejection. Another explanation for the phenomenon may be due to surface interactions between dextran and the membrane surface. Susanto et al. investigated the effect of dextran on MWCO and flux of PES and cellulose membranes.<sup>46</sup> In the investigation, exposure of PES

membranes to dextran solutions resulted in lower MWCO and a lower flux after dextran exposure. The conclusion: dextran was adsorbing onto the PES membrane surface and in the membrane pores.<sup>46</sup> Other investigations involving dextran and BSA filtrations, also yielded similar conclusions.<sup>47,48</sup> Hwang et al. challenged mixed cellulose acetate membranes with pure dextran solutions, pure BSA solutions, and a variety of mixed dextran/BSA solutions.<sup>48</sup> When compared to pure BSA solutions, pure dextran solutions resulted in higher membrane pore resistance and overall resistance. A similar conclusion was drawn: dextran was adsorbing onto the membrane surface and into the membrane pores.<sup>48</sup> Possible reasons for adsorption of dextran are electrostatic interactions between the hydroxyl groups of the cellulose groups and the hydroxyl groups of the dextran.<sup>46,48</sup> In addition to these interactions of dextran with cellulose and HEMA, there is also the possible formation of hydrogen bonding between the hydroxyl groups on the dextran and the amine groups coating the iron magnetite nanoparticles. The combination of hydrodynamic size and possible interactions of dextran with the modified membrane are reasons why BSA rejection is lower than predicted by the MWCO studies.

## 6. Conclusion

The main aim of this thesis was to extend the application of surface modified magnetically responsive membranes to UF membranes in hopes of suppressing concentration polarization effects. While it is clear that the UF membranes were successfully modified with polymer chains and then with  $\text{Fe}_3\text{O}_4$  superparamagnetic NP, the studies of the modified membranes did not conclusively prove suppression of concentration polarization. As stated in other work, the chain density and the length of the chains have a significant impact on the effect of the polymer chains.<sup>49</sup> The lack of difference in BSA and dextran rejection for modified membranes in the presence of an oscillating magnetic field indicates that the movement of the polymer chains is restricted. One possible explanation for the lack of movement may be that multiple chains are attached to the single NP through the multiple amine sites on the NP surface, which restricts movement of the NP. Another explanation may be related to the polymer chains. If the polymer chains are too densely packed this would inhibit movement and if the chains are too sparsely populated then the movement may not result in an observable effect. If the chains were too long, drag forces would inhibit movement and require a stronger magnetic field for movement. In future work, chain density and length need to be optimized. In addition, the polymerization reaction and monomer addition reactions are highly sensitive to oxidation and while oxidation of the reaction may be small, any oxidation could change the reaction rate and lead to premature termination of the chains and the polymerization reaction.<sup>21</sup> The high sensitivity to oxidation may account for the variation between membrane batches under the same conditions. Overall, the work in this thesis has proven it is possible to modify the surface of UF RC membranes with  $\text{Fe}_3\text{O}_4$  NP capped poly(HEMA) chains, but more work is needed to prove this particular magnetically responsive membrane can suppress concentration polarization.

## 7. Works Cited

1. Radcliff, B. R. & Zarnadze, A. *Application of Membrane Technology to the Production of Drinking Water*. 23–25 (2004).
2. Kulkarni, S. S., Funk, E. W. & Li, N. N. in *Membr. Handb.* (Sirkar, K. K. & Ho, W. S. W.) 393–407 (Kluwer Academic Publishers, 1992).
3. Vardanega, R. *et al.* Effect of magnetic field on the ultrafiltration of bovine serum albumin. *Bioprocess Biosyst. Eng.* 1087–1093 (2012).
4. Jönsson, A. & Trägårdh, G. Fundamental principles of ultrafiltration. *Chem. Eng. Process.* **27**, 67–81 (1990).
5. Mohammad, A. W., Ng, C. Y., Lim, Y. P. & Ng, G. H. Ultrafiltration in Food Processing Industry: Review on Application, Membrane Fouling, and Fouling Control. *Food Bioprocess Technol.* **5**, 1143–1156 (2012).
6. Ulbricht, M. Advanced functional polymer membranes. *Polym. J.* **47**, 2217–2262 (2006).
7. Sablani, S., Goosen, M., Al-Belushi, R. & Wilf, M. Concentration polarization in ultrafiltration and reverse osmosis: a critical review. *Desalination* **141**, 269–289 (2001).
8. Guo, W., Ngo, H.-H. & Li, J. A mini-review on membrane fouling. *Bioresour. Technol.* 27–34 (2012).
9. Fane, A. & Fell, C. A review of fouling and fouling control in ultrafiltration. *Desalination* **62**, 117–136 (1987).
10. Belfort, G., Davis, R. H. & Zydney, A. L. The behavior of suspensions and macromolecular solutions in crossflow microfiltration. *J. Memb. Sci.* **96**, 1–58 (1994).
11. Wandera, D., Wickramasinghe, S. R. & Husson, S. M. Stimuli-responsive membranes. *J. Membr. Sci.* **357**, 6–35 (2010).
12. Himstedt, H. H. *et al.* Magnetically activated micromixers for separation membranes. *Langmuir* **27**, 5574–81 (2011).
13. Barroso, T. *et al.* Influence of poly(N-isopropylacrylamide) and poly(N,N'-diethyl acrylamide) coatings on polysulfone/polyacrylonitrile-based membranes for protein separation. *Polym. Adv. Technol.* 1381–1393 (2011).
14. Schacher, F., Rudolph, T., Wieberger, F., Ulbricht, M. & Müller, A. H. E. Double stimuli-responsive ultrafiltration membranes from polystyrene-block-poly(N,N-

- dimethylaminoethyl methacrylate) diblock copolymers. *ACS Appl. Mater. Interfaces* **1**, 1492–503 (2009).
15. Zhao, X., Su, Y., Chen, W., Peng, J. & Jiang, Z. pH-responsive and fouling-release properties of PES ultrafiltration membranes modified by multi-functional block-like copolymers. *J. Membr. Sci.* **382**, 222–230 (2011).
  16. Cheng, C. *et al.* Remarkable pH-sensitivity and anti-fouling property of terpolymer blended polyethersulfone hollow fiber membranes. *J. Membr. Sci.* **378**, 369–381 (2011).
  17. Li, L. *et al.* Preparation and characterization of poly(acrylonitrile-acrylic acid-N-vinyl pyrrolidinone) terpolymer blended polyethersulfone membranes. *J. Membr. Sci.* **349**, 56–64 (2010).
  18. Kochkodan, V. M. & Sharma, V. K. Graft polymerization and plasma treatment of polymer membranes for fouling reduction: a review. *J. Environ. Sci. Heal. Part A Toxic/Hazard. Subst. Environ. Eng.* **47**, 1713–27 (2012).
  19. Matyjaszewski, K. & Xia, J. Atom Transfer Radical Polymerization. *Chem. Rev.* **101**, 2921 – 2990 (2001).
  20. Nanda, A. K. & Matyjaszewski, K. Effect of [bpy]/[Cu(I)] Ratio, Solvent, Counterion, and Alkyl Bromides on the Activation Rate Constants in Atom Transfer Radical Polymerization. *Macromolecules* **36**, 599–604 (2003).
  21. Matyjaszewski, K. Atom Transfer Radical Polymerization (ATRP): Current Status and Future Perspectives. *Macromolecules* **45**, 4015–4039 (2012).
  22. Adrus, N. & Ulbricht, M. Novel hydrogel pore-filled composite membranes with tunable and temperature-responsive size-selectivity. *J. Mater. Chem.* **22**, 3088 (2012).
  23. Oak, M., Kobayashi, T. & Wang, H. pH effect on molecular size exclusion of polyacrylonitrile ultrafiltration membranes having carboxylic acid groups. *J. Membr. Sci.* **123**, 185–195 (1997).
  24. Peng, T. A. O. & Cheng, Y. pH-Responsive Permeability of PE-g-PMAA Membranes. *J. Appl. Polym. Sci.* 778–786 (1999).
  25. Chung, D., Ito, Y. & Imanishi, Y. Preparation of porous membranes grafted with poly(spiropyran-containing methacrylate) and photocontrol of permeability. *J. Appl. Polym. Sci.* **51**, 2027–2033 (1994).
  26. Gorey, C. & Escobar, I. C. N-isopropylacrylamide (NIPAAm) modified cellulose acetate ultrafiltration membranes. *J. Membr. Sci.* **383**, 272–279 (2011).

27. Mondal, S. & Wickramasinghe, S. R. Photo-induced graft polymerization of N-isopropyl acrylamide on thin film composite membrane: Produced water treatment and antifouling properties. *Sep. Purif. Technol.* **90**, 231–238 (2012).
28. Wandera, D., Wickramasinghe, S. R. & Husson, S. M. Modification and characterization of ultrafiltration membranes for treatment of produced water. *J. Membr. Sci.* **373**, 178–188 (2011).
29. Yu, S. *et al.* Surface modification of thin-film composite polyamide reverse osmosis membranes with thermo-responsive polymer (TRP) for improved fouling resistance and cleaning efficiency. *Sep. Purif. Technol.* **76**, 283–291 (2011).
30. Hesampour, M., Huuhilo, T., Mäkinen, K., Mänttari, M. & Nyström, M. Grafting of temperature sensitive PNIPAAm on hydrophilised polysulfone UF membranes. *J. Membr. Sci.* **310**, 85–92 (2008).
31. Pan, K., Zhang, X. & Cao, B. Surface-initiated atom transfer radical polymerization of regenerated cellulose membranes with thermo-responsive properties. *Polym. Int.* n/a–n/a (2010). doi:10.1002/pi.2773
32. Zhao, C., Nie, S., Tang, M. & Sun, S. Polymeric pH-sensitive membranes—A review. *Prog. Polym. Sci.* **36**, 1499–1520 (2011).
33. Himstedt, H. H., Marshall, K. M. & Wickramasinghe, S. R. pH-responsive nanofiltration membranes by surface modification. *J. Membr. Sci.* **366**, 373–381 (2011).
34. Latulippe, D. R., Mika, A. M., Childs, R. F., Ghosh, R. & Filipe, C. D. M. Flux performance and macrosolute sieving behavior of environment responsive formed-in-place ultrafiltration membranes. *J. Membr. Sci.* **342**, 227–235 (2009).
35. Kotitz, R., Fannin, C. & Trahms, L. Time domain study of Brownian and Neel relaxation in ferrofluids. *J. Magn. Magn. Mater.* **149**, 42–46 (1995).
36. Savva, I. *et al.* Fabrication, Characterization, and Evaluation in Drug Release Properties of Magnetoactive Poly(ethylene oxide) – Poly(. *Biomacromolecules* (2013).
37. Ruijun, W. *et al.* Polysaccharide separation mechanism in polysulfone-Fe<sub>3</sub>O<sub>4</sub> magnetic composite membranes. *Chinese Sci. Bull.* **56**, 1951–1956 (2011).
38. Jian, P., Yahui, H., Yang, W. & Linlin, L. Preparation of polysulfone – Fe<sub>3</sub>O<sub>4</sub> composite ultrafiltration membrane and its behavior in magnetic field. *J. Memb. Sci.* **284**, 9–16 (2006).
39. Gajda, A. M. & Ulbricht, M. Magnetic Fe<sub>3</sub>O<sub>4</sub> nanoparticle heaters in smart porous membrane valves. *J. Mater. Chem.* 1317–1326 (2014). doi:10.1039/c3tb21400a



40. Himstedt, H. H., Yang, Q., Qian, X., Ranil Wickramasinghe, S. & Ulbricht, M. Toward remote-controlled valve functions via magnetically responsive capillary pore membranes. *J. Memb. Sci.* **423-424**, 257–266 (2012).
41. Yang, Q., Himstedt, H. H., Ulbricht, M., Qian, X. & Ranil Wickramasinghe, S. Designing magnetic field responsive nanofiltration membranes. *J. Memb. Sci.* **430**, 70–78 (2013).
42. Coessens, V., Pyun, J., Miller, P. J., Gaynor, S. G. & Matyjaszewski, K. Functionalization of polymers prepared by ATRP using radical addition reactions. *Macromol. Rapid Commun.* **21**, 103–109 (2000).
43. Zydney, A. L. & Xenopoulos, A. Improving dextran tests for ultrafiltration membranes: Effect of device format. *J. Memb. Sci.* **291**, 180–190 (2007).
44. Susanto, H., Franzka, S. & Ulbricht, M. Dextran fouling of polyethersulfone ultrafiltration membranes—Causes, extent and consequences. *J. Memb. Sci.* **296**, 147–155 (2007).
45. Armstrong, J. K., Wenby, R. B., Meiselman, H. J. & Fisher, T. C. The hydrodynamic radii of macromolecules and their effect on red blood cell aggregation. *Biophys. J.* **87**, 4259–70 (2004).
46. Susanto, H. & Ulbricht, M. Influence of ultrafiltration membrane characteristics on adsorptive fouling with dextrans. *J. Memb. Sci.* **266**, 132–142 (2005).
47. Yao, M., Zhang, K. & Cui, L. Characterization of protein–polysaccharide ratios on membrane fouling. *Desalination* **259**, 11–16 (2010).
48. Hwang, K.-J. & Chiang, Y.-C. Comparisons of membrane fouling and separation efficiency in protein/polysaccharide cross-flow microfiltration using membranes with different morphologies. *Sep. Purif. Technol.* **125**, 74–82 (2014).
49. Wandera, D., Himstedt, H. H., Marroquin, M., Wickramasinghe, S. R. & Husson, S. M. Modification of ultrafiltration membranes with block copolymer nanolayers for produced water treatment: The roles of polymer chain density and polymerization time on performance. *J. Memb. Sci.* **403-404**, 250–260 (2012).

## 8. Appendices

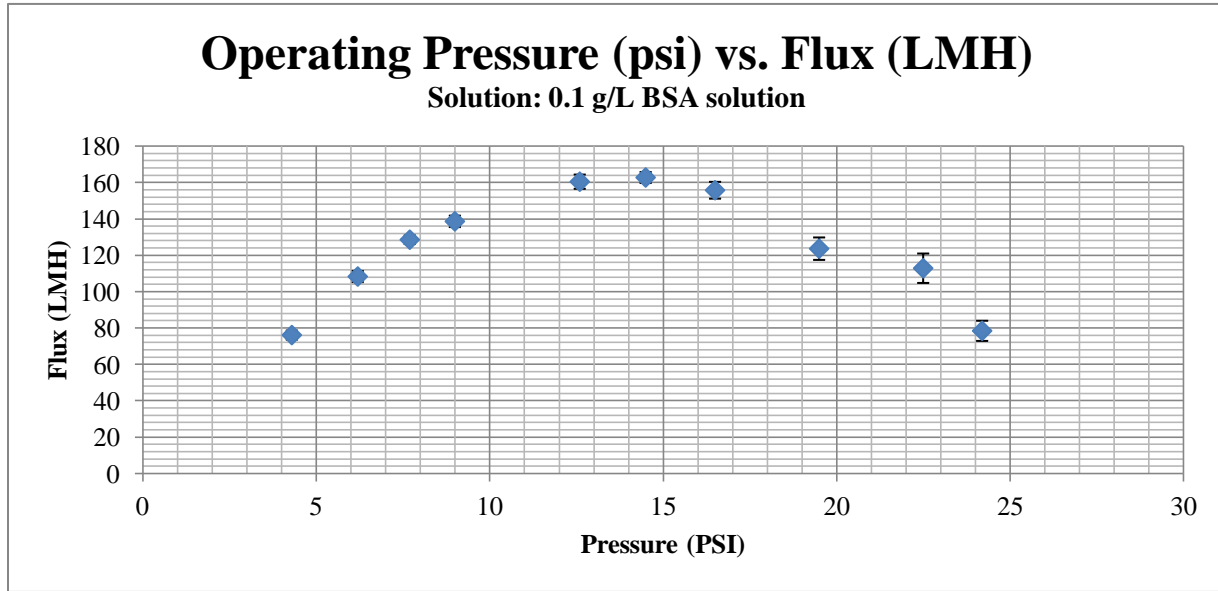


Figure 17: Operating Pressure (psi) vs. Flux (LMH) that was used to determine the critical pressure and the best operating pressure for the 0.1 g/L BSA filtration experiments.

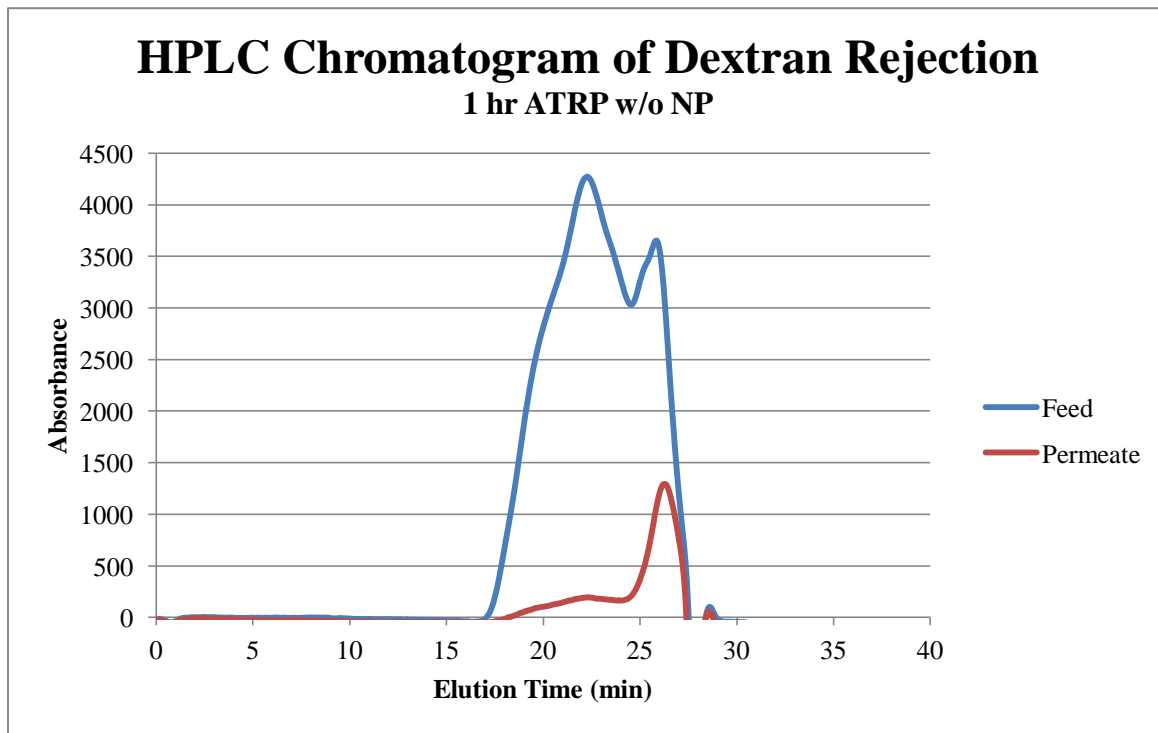


Figure 18: Dextran HPLC chromatogram for the 1 hour ATRP modified membrane.

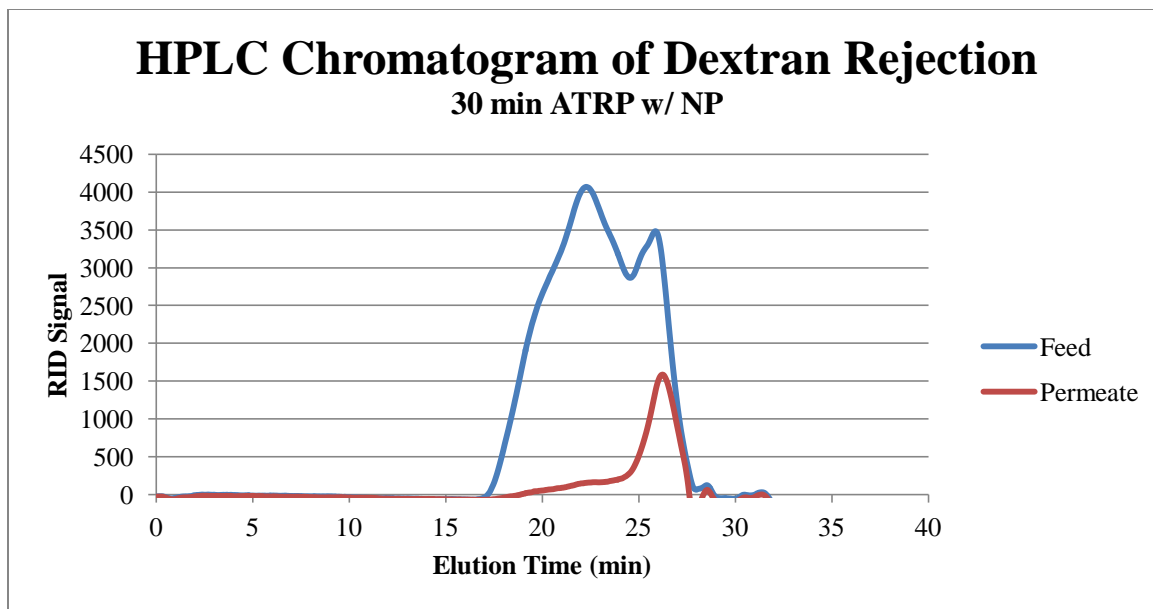


Figure 19: Dextran HPLC chromatogram for the 30 min ATRP - NP modified membrane.

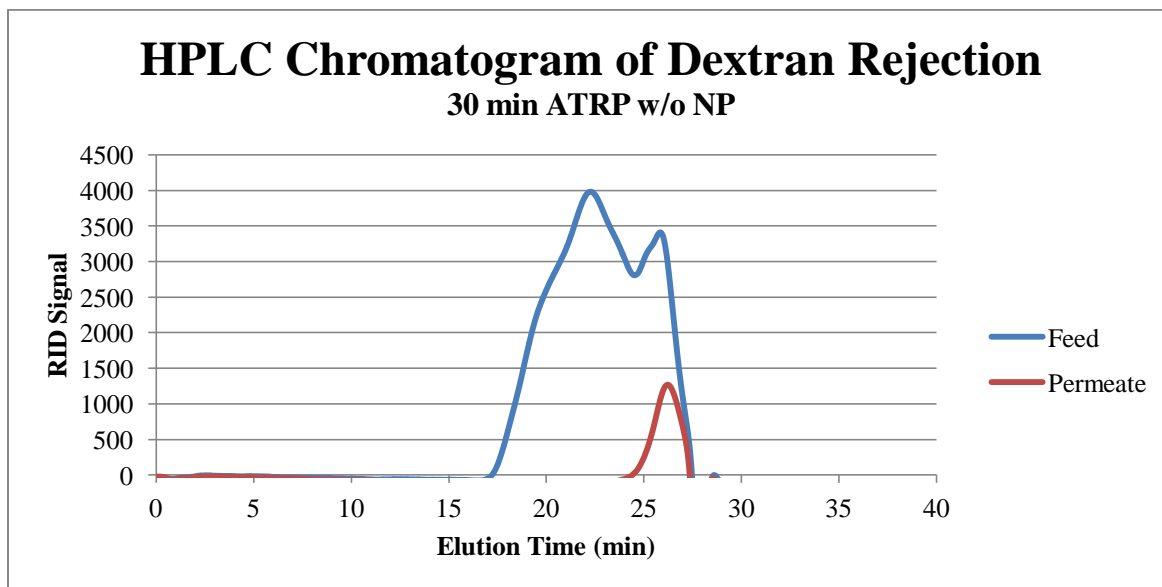


Figure 20: Dextran HPLC chromatogram for the 30 min hr ATRP without NP modified membrane.

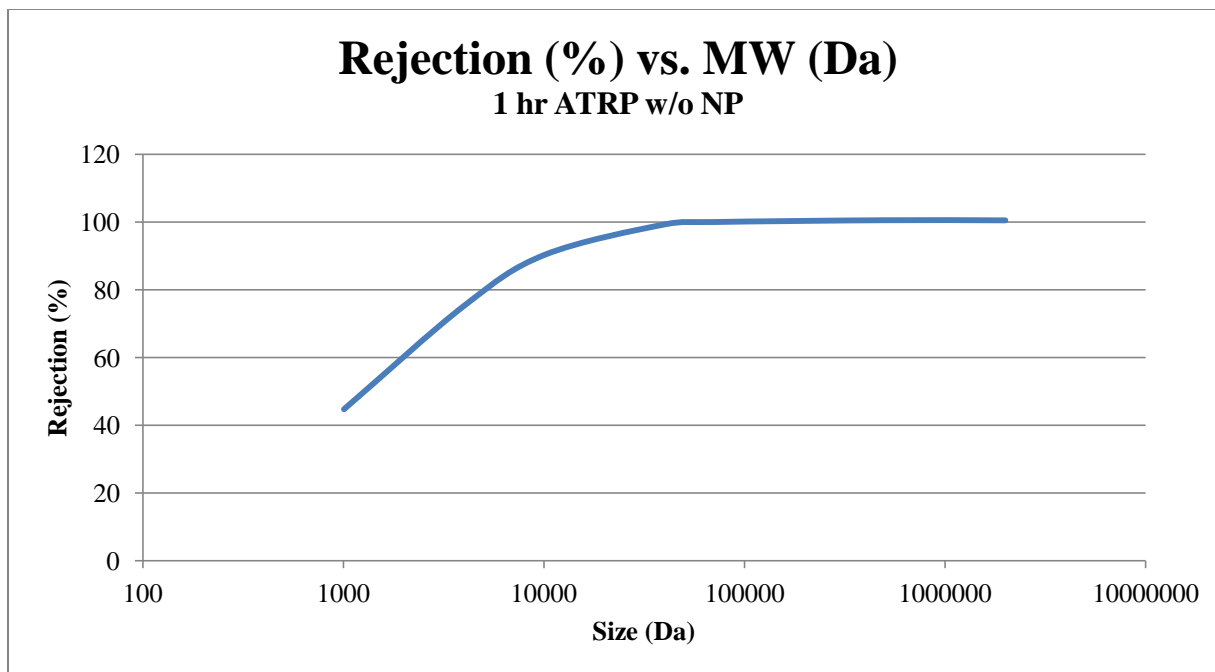


Figure 21: Rejection vs. MW curve used to determine MWCO for 1 hr ATRP without NP modified membrane.

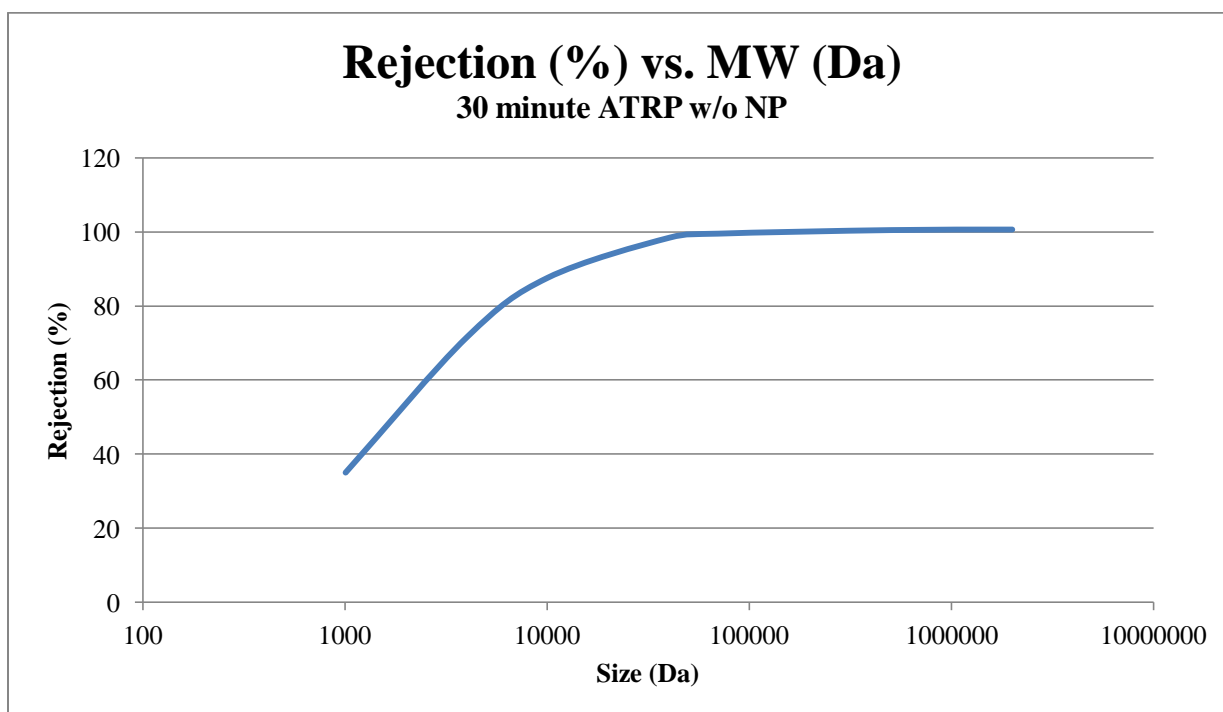


Figure 22: Rejection vs. MW curve used to determine MWCO for 30 minute ATRP without NP modified membrane.

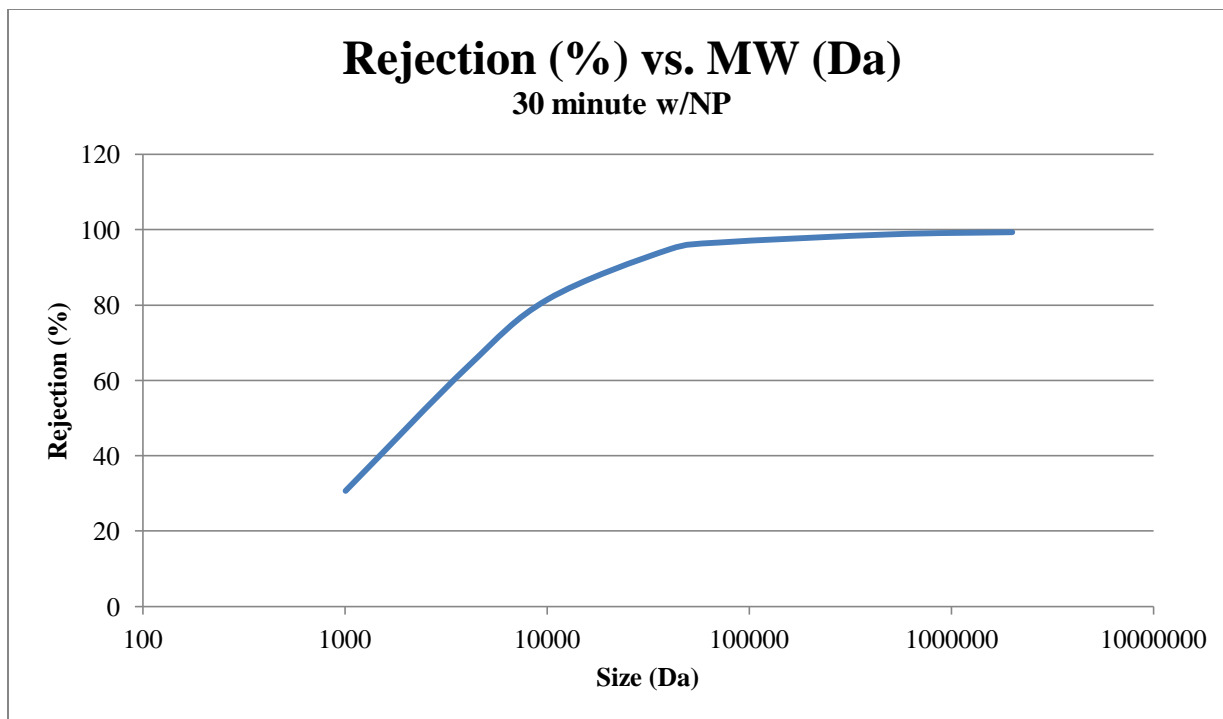


Figure 23: Rejection vs. MW curve used to determine MWCO for 30 minute ATRP - NP modified membrane.